



**HAL**  
open science

# Detrimental Effect and Neutralization of in Situ Produced Water on Zirconia Nanoparticles Obtained by a Nonaqueous Sol–Gel Method

Jess Gambe, Fabien Remondiere, Jenny Jouin, Laura Portal, Philippe Thomas, Olivier Masson

► **To cite this version:**

Jess Gambe, Fabien Remondiere, Jenny Jouin, Laura Portal, Philippe Thomas, et al.. Detrimental Effect and Neutralization of in Situ Produced Water on Zirconia Nanoparticles Obtained by a Nonaqueous Sol–Gel Method. *Inorganic Chemistry*, 2019, 58 (22), pp.15175-15188. 10.1021/acs.inorgchem.9b02076 . hal-02433804

**HAL Id: hal-02433804**

**<https://unilim.hal.science/hal-02433804v1>**

Submitted on 26 Nov 2020

**HAL** is a multi-disciplinary open access archive for the deposit and dissemination of scientific research documents, whether they are published or not. The documents may come from teaching and research institutions in France or abroad, or from public or private research centers.

L'archive ouverte pluridisciplinaire **HAL**, est destinée au dépôt et à la diffusion de documents scientifiques de niveau recherche, publiés ou non, émanant des établissements d'enseignement et de recherche français ou étrangers, des laboratoires publics ou privés.

This document is confidential and is proprietary to the American Chemical Society and its authors. Do not copy or disclose without written permission. If you have received this item in error, notify the sender and delete all copies.

**Detrimental effect and neutralization of in situ produced water on zirconia nanoparticles obtained by a nonaqueous sol-gel method**

Journal:	<i>Inorganic Chemistry</i>
Manuscript ID	ic-2019-02076t.R2
Manuscript Type:	Article
Date Submitted by the Author:	16-Oct-2019
Complete List of Authors:	Gambe, Jess; Institut de Recherche sur les Céramiques REMONDIERE, Fabien; Institut de Recherche sur les Céramiques Jouin, Jenny; Institut de Recherche sur les Céramiques Portal, Laura; Institut de Recherche sur les Céramiques Thomas, Philippe; Institut de Recherche sur les Céramiques Masson, Olivier; Institut de Recherche sur les Céramiques

SCHOLARONE™  
Manuscripts

1  
2  
3  
4  
5  
6  
7  
8  
9  
10  
11  
12  
13  
14  
15  
16  
17  
18  
19  
20  
21  
22  
23  
24  
25  
26  
27  
28  
29  
30  
31  
32  
33  
34  
35  
36  
37  
38  
39  
40  
41  
42  
43  
44  
45  
46  
47  
48  
49  
50  
51  
52  
53  
54  
55  
56  
57  
58  
59  
60

# Detrimental effect and neutralization of *in-situ*-produced water on zirconia nanoparticles obtained by a nonaqueous sol-gel method

*Jess Gambe, Fabien Rémondière \*, Jenny Jouin, Laura Portal, Philippe Thomas and Olivier  
Masson*

Institute of Research for Ceramics (IRCER), UMR 7315 CNRS, Université de Limoges, Centre  
Européen de la Céramique, 12 rue Atlantis, 87068 Limoges Cedex, France

**KEYWORDS:** Zirconia nanoparticles, nonaqueous sol-gel route, alcohol dehydration, *in-situ*  
water production.

## Supporting Information

**ABSTRACT:** In this work, the phase purity and size of zirconia nanocrystals samples were studied in terms of zirconium concentration, added water content and subsequent use of a post solvothermal treatment. The progressive tetragonal-to-monoclinic transformation of zirconia sample was observed to be strongly related to the water content of the alcoholic medium. But more surprisingly, it has been shown that even under initially anhydrous conditions and for particle size below 5 nm, the phase purity of the samples was deteriorated by a side-reaction of alcohol dehydration catalyzed by the surface of the nanoparticles (NPs). Since the phase transformation is essentially driven by the water content of the reaction mixture, we have shown that it was possible to recover an excellent phase purity without the help of any usual dopants

1  
2  
3 by adding a strong alkaline desiccating agent. Provided that a sufficient sodium to zirconium  
4 ratio was ensured, the formation of the monoclinic phase was not observed whatever the  
5 zirconium precursor concentration. The effectiveness of this cure was related to the ability of  
6 zirconium precursor concentration. The effectiveness of this cure was related to the ability of  
7 sodium metal to generate reactive alkoxide able to neutralize water and to catalyze an  
8 alternative sol-gel mechanism leading to the formation of the t-ZrO<sub>2</sub> NPs.  
9  
10  
11  
12  
13  
14  
15  
16  
17

## 18 I. INTRODUCTION

21 Zirconia ZrO<sub>2</sub> is a ceramic oxide with three usual polymorphs at standard pressure, *i.e.*,  
22 monoclinic (m), tetragonal (t), and cubic (c). In the bulk, zirconia is stable as the monoclinic  
23 phase at room temperature and then, as the temperature increases, it transforms into the  
24 tetragonal phase (1170°C < T < 2370°C) and, eventually, into the cubic phase above 2370°C.<sup>1</sup>  
25 The cubic phase has the fluorite structure, and the other polymorphs are distorted versions of  
26 this structure. Zirconia finds application in many technologies, e.g. solid-state gas sensors,  
27 electrolytes for solid oxide fuel cells, thermal barriers, structural material, catalysis...<sup>2-5</sup> In most  
28 of these applications, zirconia must be stabilized at room temperature in the tetragonal or cubic  
29 form. This can be achieved by two methodologies: (i) by incorporating cation dopants – the  
30 inclusion of a divalent, trivalent or tetravalent cation of a size different from that of Zr<sup>4+</sup> (e.g.  
31 Mg<sup>2+</sup>, Ca<sup>2+</sup>, Y<sup>3+</sup>, Ce<sup>4+</sup>) induces the apparition of oxygen vacancies that stabilizes the high  
32 symmetry phases; and (ii) by limiting the crystallite size below the critical size which induces  
33 the stabilization of the metastable polymorph at room temperature due to differences in surface  
34 energies.<sup>1,6-9</sup> Garvie predicted that pure ZrO<sub>2</sub> could be stabilized in the tetragonal structure at  
35 room temperature when the spherical particle size is less than 30 nm. Such effect has been  
36 experimentally shown by many authors.<sup>10-14</sup> As a catalyst, ZrO<sub>2</sub> has been selected due to its  
37 specific amphoteric behavior and large thermal stability in order to catalyze reactions including  
38  
39  
40  
41  
42  
43  
44  
45  
46  
47  
48  
49  
50  
51  
52  
53  
54  
55  
56  
57  
58  
59  
60

1  
2  
3 the dehydration and dehydrogenation of alcohols, hydrogenation and isomerization of olefins.  
4  
5 Among the usual polymorphs, the tetragonal polymorph t-ZrO<sub>2</sub> is believed to possess the  
6  
7 highest catalytic activity.<sup>15-21</sup>  
8  
9

10 For the preparation of inorganic materials with well-defined morphologies, soft chemistry  
11  
12 syntheses are preferred to the solid-state chemistry methodology. Over the past two decades,  
13  
14 several chemical methods have been developed for the preparation of zirconia nanocrystals,  
15  
16 including sol-gel, thermal decomposition, aqueous precipitation with or without hydrothermal  
17  
18 treatment, and recently a two-phase approach based on the phase transfer and a separation  
19  
20 mechanism.<sup>22</sup> Another possible general method is the nonhydrolytic sol-gel route successfully  
21  
22 employed in the presence of surfactant by Joo *et al.* or via a glycothermal treatment by Inoue  
23  
24 *et al.* or via a surfactant-free route by Garnweitner *et al.*<sup>23-27</sup> There are many ways to prepare  
25  
26 ZrO<sub>2</sub> particles, but solvothermal methods have attracted more attention in recent years,  
27  
28 especially the benzyl alcohol route, which is a surfactant-free but solvent-controlled route  
29  
30 enabling the production of high purity compounds with good control over the particle size, the  
31  
32 surface properties, and the assembly behavior.<sup>28</sup>  
33  
34  
35  
36

37 During the solvothermal synthesis of nanoparticles, even if the precursors, the additives and  
38  
39 the solvent are water-free, it is not impossible that some water is produced by secondary  
40  
41 reactions and mainly contributes to the formation mechanism of the final oxide nanoparticles;  
42  
43 indeed, the presence of water has been detected in various chemical systems and authors prefer  
44  
45 thus to refer to the denomination of nonaqueous sol-gel route.<sup>29-34</sup> Moreover, the produced-  
46  
47 water is known to be able to activate the condensation of metallic precursors or clusters and to  
48  
49 initiate the crystallization of metal oxide nanoparticles. Only a few articles are focused on the  
50  
51 potential effect of water during synthesis and studied its influence on the precursor  
52  
53 condensation, the size of the final nanoparticles and more importantly, the polymorphic variety  
54  
55 that results.<sup>35</sup>  
56  
57  
58  
59  
60

1  
2  
3 In this paper, we present the effect of *in-situ* formation of water, which degrades the phase  
4 purity and the size control of zirconia nanoparticles obtained by the nonaqueous benzyl alcohol  
5 route developed by Garnweitner.<sup>26</sup> In a first part, we investigate the effect of the zirconium  
6 precursor concentration, the water content intentionally introduced into the reaction mixture  
7 and finally, the subsequent addition of a post-solvothermal treatment onto as-synthesized NPs.  
8 In a second part, we study the use of a reactive sodium alkoxide as an effective cure against the  
9 detrimental effect of water on the sample phase purity. The possible roles of sodium cations  
10 and alkoxide species are finally discussed and taken in account to propose an original NP  
11 formation pathway.  
12  
13  
14  
15  
16  
17  
18  
19  
20  
21  
22  
23  
24  
25

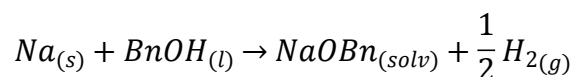
## 26 II. EXPERIMENTAL SECTION

27  
28

29 All chemicals were stored and used as received in a dried-air flow glovebox. Water in the  
30 solvents was titrated by the Karl Fischer method and all the solvents were found to be strictly  
31 anhydrous. For the solvothermal treatment, Berghof digestion bombs were used with 25 mL  
32 inner volume Teflon cup.  
33  
34  
35  
36  
37

38 Two series of samples have been synthesized and differ essentially by the presence or absence  
39 of a sodium precursor. The experimental conditions are summarized in Table 1. The first series  
40 of samples was prepared by introducing 1, 4 or 32 mmol of zirconium isopropoxide isopropanol  
41 adduct  $[\text{Zr}(\text{O}^i\text{Pr})_4 \cdot \text{HO}^i\text{Pr}]_2$  (Aldrich, 99.9%) and 12.5 mL of anhydrous benzyl alcohol BnOH  
42 (Aldrich, 99.8% anhydrous) into a Teflon reactor. For selected cases, the syntheses were  
43 repeated in aqueous conditions with the use of a mixed solvent (deionized water and benzyl  
44 alcohol) in replacement of pure anhydrous benzyl alcohol. In addition, the effect of a  
45 solvothermal post-treatment for 48 hours at 210°C in anhydrous or partially benzyl alcohol  
46 medium, namely with an aqueous fraction of 5, 20 and 50 vol.%, was tested on nanoparticles  
47 prepared with the initial anhydrous conditions. The second series of samples were produced *via*  
48  
49  
50  
51  
52  
53  
54  
55  
56  
57  
58  
59  
60

1  
2  
3 an alternate procedure consisting in adding the predissolution step of a sodium precursor,  
4 namely sodium metal Na (Alfa Aesar, 99.95%), sodium isopropoxide Na<sup>i</sup>OPr (Alfa Aesar,  
5 99%) or sodium chloride NaCl (Alfa Aesar, puratronic 99.998%). It is important to note that  
6 unlike Na<sup>i</sup>OPr which is soluble for a concentration of 0.20 mol.L<sup>-1</sup>, NaCl is only poorly soluble  
7 into benzyl alcohol and was directly added to the initial zirconium alkoxide benzyl alcohol  
8 mixture. The dissolution of sodium metal in benzyl alcohol (BnOH) occurred at room  
9 temperature under the slow release of hydrogen gas as it is shown in the following redox  
10 reaction:  
11  
12  
13  
14  
15  
16  
17  
18  
19  
20



21  
22  
23  
24  
25 NaCl and Na<sup>i</sup>OPr were used with a solute concentration of 0.20 mol.L<sup>-1</sup> whereas the sodium  
26 benzoate solution produced in the case of sodium metal and benzyl alcohol was studied for  
27 various concentrations, *i.e.* 0.05, 0.10, 0.20, 0.40 or 1.00 mol.L<sup>-1</sup>. A volume of 12.5 mL of the  
28 prepared sodium-based solution was then used as solvent in addition to zirconium isopropoxide  
29 isopropanol adduct (4 mmol).  
30  
31  
32  
33  
34  
35

36  
37 Whatever the initial reaction mixture (series 1 or 2), the Teflon reactor was inserted and sealed  
38 into the inox steel bomb, and heated up to 210°C for 48 hours *via* a pre-heated isothermal  
39 apparatus disposed on a hot plate. After cooling, the milky suspension was centrifuged and the  
40 precipitate was washed three times thoroughly with 20 mL anhydrous ethanol, dispersed in  
41 dichloromethane and finally air-dried over the night at room temperature.  
42  
43  
44  
45  
46  
47

48  
49 The obtained samples were characterized by the following techniques: X-ray powder  
50 diffraction (XRD), transmission electron microscopy (TEM), selected area electron diffraction  
51 (SAED), thermogravimetric analysis (TG), <sup>1</sup>H- and <sup>13</sup>C-based nuclear magnetic resonance  
52 (NMR) in the case of the study of the supernatant diluted in DMSO-d<sub>6</sub> and elemental analysis  
53 using inductively coupled mass spectroscopy (ICP-MS). The XRD diagrams of all the samples  
54  
55  
56  
57  
58  
59  
60

were collected using a Bruker D8 Advance diffractometer, operating in the Bragg-Brentano configuration using Cu K $_{\alpha 1}$  radiation ( $\lambda = 1.54 \text{ \AA}$ ) from  $10^\circ$  to  $110^\circ$ . The size, morphology and distribution in size of the samples were analyzed using a JEOL JEM-2100F microscope at an accelerating voltage of 200 kV. Specimens for the TEM studies were prepared by depositing a drop of diluted suspensions onto a 400 mesh copper grid, coated with an ultrathin lacey carbon film. Prior to deposition, the suspensions were sonicated for 2 min to avoid excessive aggregation and diluted into dichloromethane ( $\text{CH}_2\text{Cl}_2$ ) in the presence of oleic acid. The thermogravimetric analyses were performed on a Netzsch instrument (model STA 449F3, Germany) and carried out from  $25^\circ\text{C}$  to  $800^\circ\text{C}$  at a heating rate of  $10^\circ\text{C}\cdot\text{min}^{-1}$  in flowing argon gas ( $20 \text{ mL}\cdot\text{min}^{-1}$ ). ICP-MS was accomplished using a Perkin-Elmer Sciex Elan 6100 instrument to evaluate the relative amount of sodium compared to zirconium. Prior to the elemental analysis, the nanoparticles were first calcined at  $900^\circ\text{C}$  and then dissolved using a microwave-assisted digester in the presence of concentrated sulfuric, nitric and hydrofluoric acids. The resulted solutions were then diluted in the presence of boric acid to enhance the solutions stability.

**Table 1.** Experimental conditions used for the synthesis of zirconia nanoparticles prepared at  $210^\circ\text{C}$  for 48 hours with zirconium isopropoxide-isopropanol adduct in anhydrous benzyl alcohol (or aqueous benzyl alcohol), monoclinic phase content and average nanoparticles size.

[Zr]	Sodium source	[Na]	[Na]/[Zr]	Added water	Solvothermal post-treatment	m-ZrO $_2$ content	NPs size	
(mol.L $^{-1}$ )		(mol.L $^{-1}$ )		(vol.%)	Temp./time	water content (vol.%)	(wt.%)	(nm)
0.08	none	0	0	0	none	none	37	3.3
0.32	none	0	0	0	none	none	44	3.7
1.28	none	0	0	0	none	none	74	4.5
0.32	none	0	0	5	none	none	51	5.2



0.32	none	0	0	10	none	none	59	6.5
0.32	none	0	0	20	none	none	58	7.0
0.32	none	0	0	0	210°C/48h	0	41	3.7
0.32	none	0	0	0	210°C/48h	5	57	3.9
0.32	none	0	0	0	210°C/48h	20	84	4.3
0.32	none	0	0	0	210°C/48h	50	89	5.0
0.32	Na metal	0.05	0.156	0	none	none	40	3.7
0.32	Na metal	0.10	0.312	0	none	none	23	3.4
0.32	Na metal	0.20	0.625	0	none	none	0	3.2
0.32	Na metal	0.40	1.25	0	none	none	0	4.8
0.32	Na metal	1.00	3.125	0	none	none	0	-
0.32	NaO <sup>i</sup> Pr	0.20	0.625	0	none	none	0	-
0.32	NaCl	0.20	0.625	0	none	none	-	-
1.28	Na metal	0.20	0.156	0	none	none	-	-
1.28	Na metal	0.80	0.625	0	none	none	0	-

### III. RESULTS AND DISCUSSION

#### III.1. Detrimental effect of water on zirconia nanocrystals

##### a) Effect of zirconium isopropoxide concentration on sample phase purity

Three syntheses were carried out in anhydrous benzyl alcohol with different amounts of zirconium isopropoxide isopropanol adduct of respectively 0.08, 0.32 and 1.28 mol.L<sup>-1</sup>. The XRD diagrams of the samples are shown in the Figure 1. The three samples are clearly crystallized and the peak broadening indicates the nanocrystalline nature of the particles. For the sample obtained with the lowest concentration (Figure 1(a)), the main peaks can be attributed to the tetragonal phase, denoted here t-ZrO<sub>2</sub>, (space group P4<sub>2</sub>/nmc - JCPDS 00-050-1089). However, since the tetragonal phase of zirconia is slightly distorted with respect to the

fluorite cubic phase (for bulk  $\text{ZrO}_2$ , the  $c/a$  ratio is only 1.023, very close to the cubic ideal value of 1.0) it is very difficult to distinguish between these the tetragonal phase and a pseudo-cubic one. The extra peaks at  $2\theta = 24.0^\circ$ - $24.5^\circ$ ,  $40.7^\circ$ - $41.3^\circ$  and  $44.8^\circ$ - $45.5^\circ$  unambiguously evidences the presence of the monoclinic polymorph  $m\text{-ZrO}_2$  (Baddeleyite  $P2_1/a$  – JCPDS 00-037-1484) which cannot explain by itself all the peaks of the diagram. Moreover, the peaks intensity of  $m\text{-ZrO}_2$  is becoming more pronounced as the concentration of zirconium isopropoxide increases from 0.08 up to  $1.28 \text{ mol.L}^{-1}$  (Figure 1(a-c)).

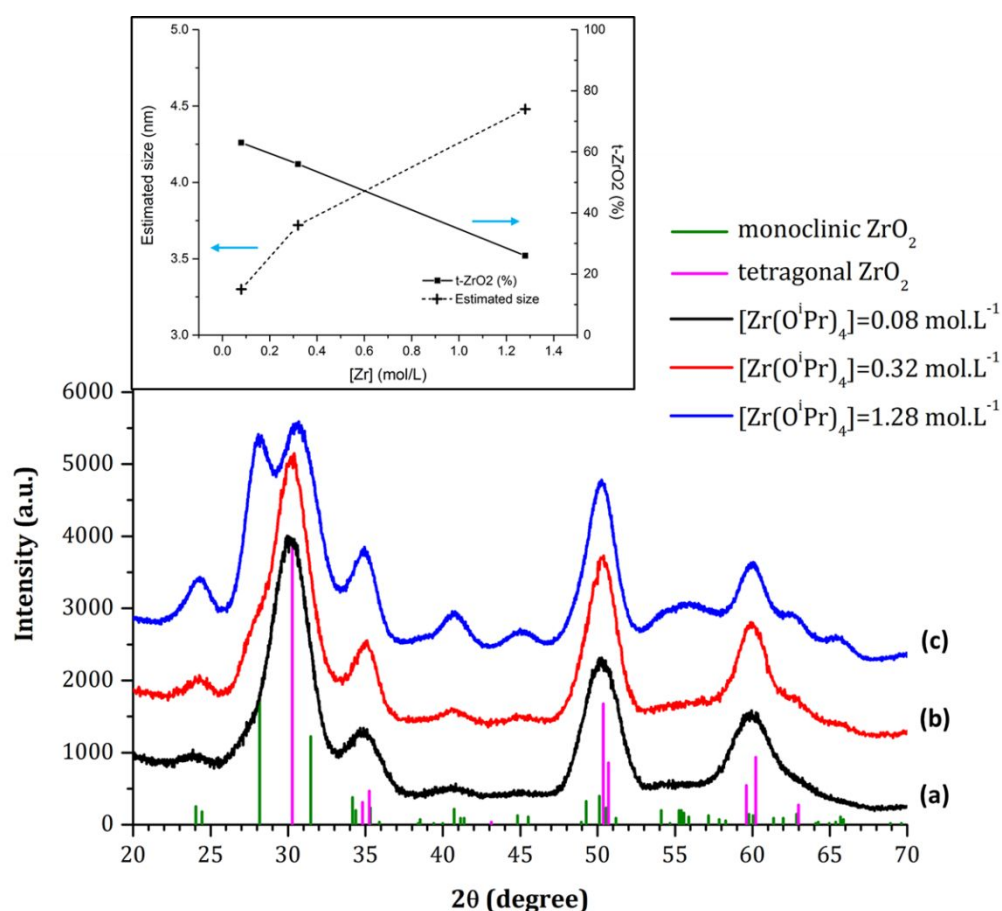


**Figure.1.** X-ray diffraction patterns of  $\text{ZrO}_2$  nanoparticles prepared by the Na-free benzyl alcohol sol-gel route with various zirconium isopropoxide concentrations of (a)  $0.08 \text{ mol.L}^{-1}$ , (b)  $0.32 \text{ mol.L}^{-1}$  and (c)  $1.28 \text{ mol.L}^{-1}$ . Also shown are the estimated size and  $t\text{-ZrO}_2$  weight fraction (inset).

In order to determine the average crystallite size and to evaluate the relative proportion of each phases, a Rietveld refinement was performed for the three samples. Due to the large peaks

1  
2  
3 broadening and overlap the refined peak profile and width parameters were constrained to be  
4 equal during the calculation assuming the same particle size for both t- and m-ZrO<sub>2</sub> phases.  
5  
6 This assumption on the crystallite size will be accredited by the TEM study of the sample. The  
7  
8 addition of microstrains is not needed to perform the Rietveld refinement. An example of  
9  
10 refinement is given in the Figure 2(a) and the global results are gathered in the Table 1. The  
11  
12 average crystallite size was found to be 3.3 nm (37 wt.% of m-ZrO<sub>2</sub>), 3.7 nm (44 wt.% of m-  
13  
14 ZrO<sub>2</sub>) and 4.5 nm (74 wt.% of m-ZrO<sub>2</sub>) for the concentration of 0.08 mol.L<sup>-1</sup>, 0.32 mol.L<sup>-1</sup> and  
15  
16 finally 1.28 mol.L<sup>-1</sup> respectively. These results indicate a significant and strong dependence of  
17  
18 the precursor concentration on the resulting nanoparticle size and the relative fraction of each  
19  
20 polymorphs. Even the use of a quite low concentration in zirconium isopropoxide is not  
21  
22 sufficient to guaranty a good phase purity of the resulting nanoparticles. TEM investigation was  
23  
24 undertaken on the sample prepared with a nominal zirconium isopropoxide concentration of  
25  
26 0.32 mol.L<sup>-1</sup>; the Figure 2(b) corresponds to the analysis of the wet particles dispersed onto an  
27  
28 ultra-thin carbon membrane. The overview micrograph of the grid at intermediate magnification  
29  
30 illustrates that the wet particles entirely consist of monodisperse objects measuring a few  
31  
32 nanometers. The inset image exhibits a crystallized nanoparticle measuring 3.8 nm. The average  
33  
34 particle diameter measured on the large overview is estimated to 3.5 +/- 0.5 nm and close to the  
35  
36 Rietveld calculation.  
37  
38  
39  
40  
41  
42  
43  
44  
45  
46  
47  
48  
49  
50  
51  
52  
53  
54  
55  
56  
57  
58  
59  
60

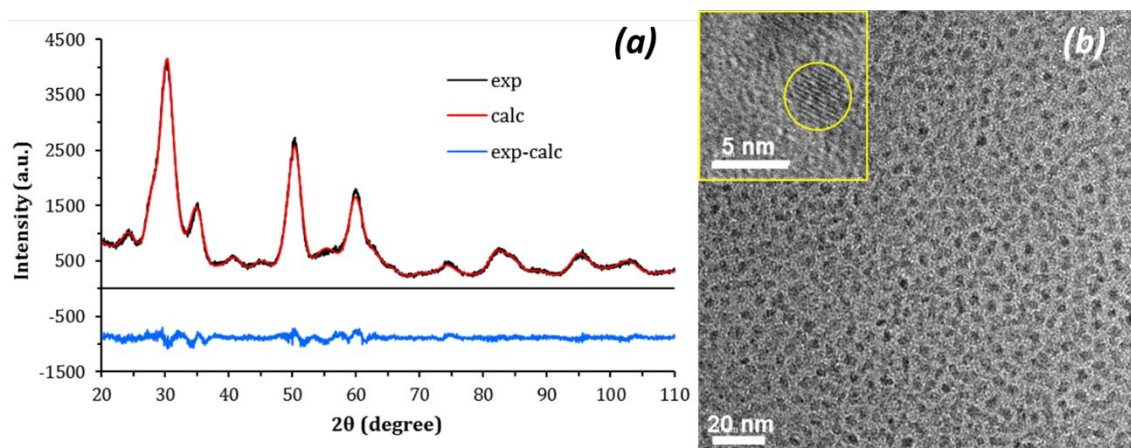


**Figure.2.** Rietveld refinement of the XRD pattern of the sample prepared by the Na-free benzyl alcohol sol-gel route with a nominal concentration in zirconium isopropoxide of  $0.32 \text{ mol.L}^{-1}$  (a) and TEM micrograph of the wet nanoparticles dispersed onto a ultra-thin carbon membrane (inset: HRTEM view of a single crystallized nanoparticle) (b).

Niederberger and coworkers have shown that the investigation of nanoparticle formation has to be considered from both the inorganic and the organic sides. In that perspective, the supernatant liquid corresponding to the reference  $0.32 \text{ mol.L}^{-1}$  sample was collected after centrifugation and subjected to  $^{13}\text{C}$ - and  $^1\text{H}$ -NMR analyses revealing the major presence of benzyl alcohol and isopropanol, and in smaller amounts the presence of benzyl and diisopropyl ethers and water (Figure.S1. in supporting information). The presence of ethers is consistent with the results of Garnweitner *et al.* indicating that the main source for zirconia formation is an ether-elimination condensation mechanism.<sup>26</sup> Besides the residual alcohols and the resulting ethers, the presence of water is quite surprising for a nonaqueous solvothermal route based on an aprotic condensation reaction and was confirmed by a positive copper (II) sulfate test. Since the main condensation mechanism proposed by Garnweitner *et al.* is a two-step process involving ligand exchange reaction in the presence of large excess of benzyl alcohol and second, aprotic ether-elimination, no formal water can be released and no hydroxyl group appears during the formation of the oxidic network. Among the other possible condensation reactions that have been observed and referenced by Niederberger, just a few of them occur *via*

1  
2  
3 the formation of hydroxylated species and thus the possible release of water, *i.e.* either the  
4 thermal decomposition of isopropoxide ligands, metal halide reaction with alcohols, aldol  
5 condensation or the C-C coupling of isopropoxide ligand with benzyl alcohol analogously to  
6 what occurs in Guerbet reaction. In the absence of zirconium halide or ketones, we can restrain  
7 the perimeter to thermal decomposition and C-C coupling reactions.<sup>34</sup> Since the thermal  
8 decomposition of metal alkoxide necessitates the use of a temperature as high as 350°C, we can  
9 exclude such eventuality in our case. The C-C coupling of benzyl alcohol and isopropoxide  
10 ligand resulting in the formation of hydroxylated species cannot be evocated to supply the  
11 formal water because on the one hand zirconium alkoxides are not known to exhibit a high  
12 Lewis acidity contrary to yttrium cation and on the other hand no coupling products of isopropyl  
13 and benzyl alcohol (e.g. 4-phenyl-2-butanol) were found in the supernatant.<sup>36-38</sup>

14  
15  
16  
17  
18  
19  
20  
21  
22  
23  
24  
25  
26  
27  
28  
29  
30  
31  
32  
33  
34  
35  
36  
37  
38  
39  
40  
41  
42  
43  
44  
45  
46  
47  
48  
49  
50  
51  
52  
53  
54  
55  
56  
57  
58  
59  
60

If water is not produced by the condensation reaction leading to the formation of the zirconia nanoparticles, it is necessary to take in account some plausible parasitic reactions with the solvent. Commonly the alcohols dehydrate in the presence of a strong acid to form either ethers at low temperatures, e.g. Williamson ether synthesis, or alkenes at higher temperatures. Inspired by the work of Kotestkyy, we propose that the water could also originate from the dehydration of the alcoholic medium mediated by the catalytic properties of the growing surface of the zirconia *nuclei* or surface of zirconia nanocrystals.<sup>39</sup> Kotestkyy *et al.* proposed the following sequence in the case of the Lewis-acid catalyzed dehydration of simple alcohols on various simple metal oxide like TiO<sub>2</sub>, ZrO<sub>2</sub> and  $\gamma$ -Al<sub>2</sub>O<sub>3</sub>: (i) alcohol adsorption on the Lewis acid metal site, (ii)  $\beta$ -hydrogen transfer to a surface O, (iii) alkene formation and desorption, (iv) water formation, desorption and catalyst regeneration. In the present case, intermolecular dehydration for benzyl alcohol and inter- and/or intramolecular dehydration for isopropanol could be evocated to argue the release of water during the solvothermal treatment.<sup>40-41</sup> Since ethers were found in minor proportion in the supernatant we can exclude the intermolecular dehydration of

1  
2  
3 alcohols and focus our attention on the intramolecular dehydration of isopropanol supported by  
4 the nanoparticle surface. Isopropanol provided by the isopropoxide-isopropanol adduct or  
5 issued from the ligand exchange reaction with benzyl alcohol seems to interact with an acid-  
6 base couple site of the oxidic catalyst, namely the zirconia nanoparticles, to dehydrate into water  
7 and volatile propene which eliminates at the opening of the reactor.  
8  
9  
10  
11  
12  
13  
14  
15  
16

### 17 **b) Detrimental effect of water on sample purity**

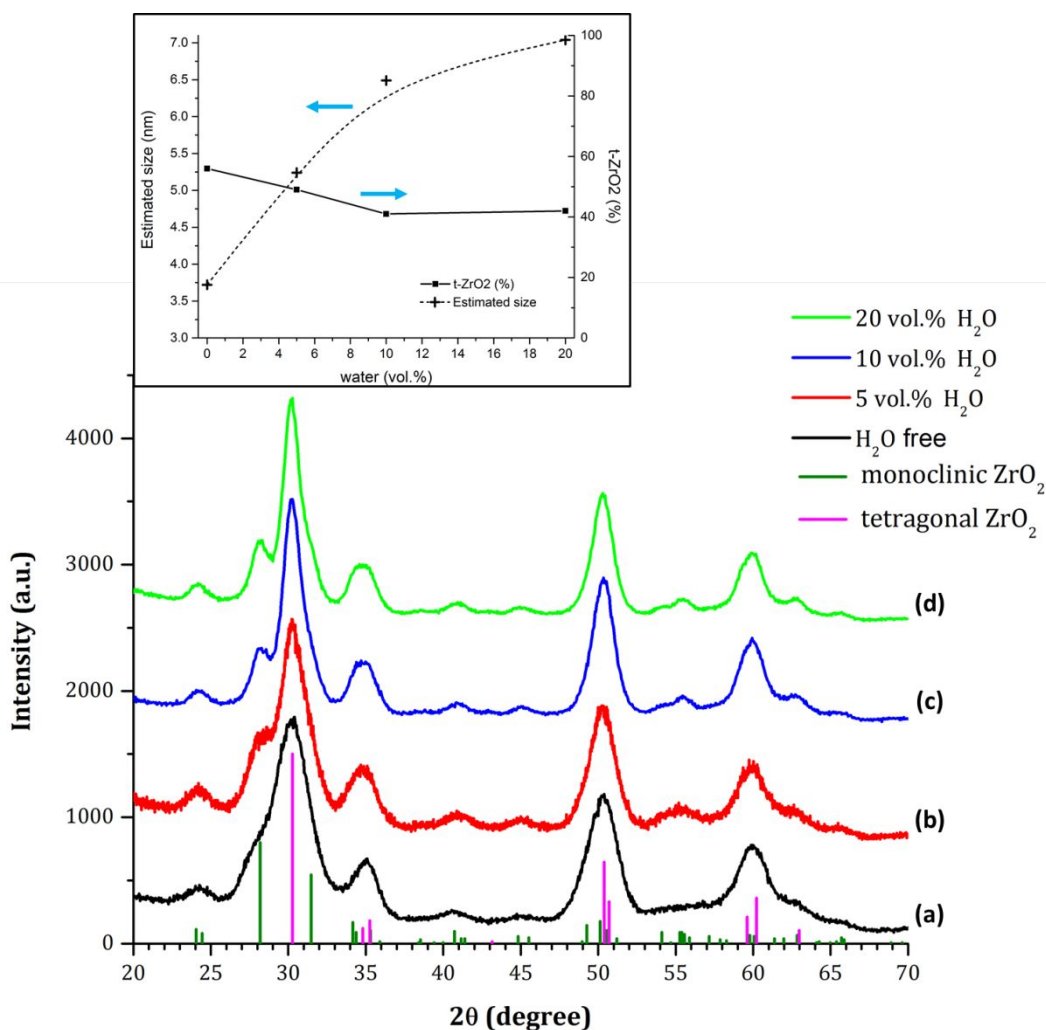
18  
19

20 In order to investigate whether the presence of *in situ* water has a significant impact on the  
21 stabilization or the formation of the monoclinic polymorph of zirconia in the final product, we  
22 decided to perform two series of experiments: (i) an intentional addition of water into the initial  
23 reaction mixture, (ii) a subsequent solvothermal treatment of the as-synthesized wet  
24 nanoparticles in regenerated anhydrous or partially hydrated benzyl alcohol.  
25  
26  
27  
28  
29  
30

31 The first series of syntheses were performed with the preliminary addition of 5, 10 and 20  
32 vol.% of deionized water in benzyl alcohol. The XRD diagrams of the resulting samples are  
33 gathered in the Figure 3. By increasing the content of water in the initial reaction mixture, we  
34 observe a modification in the peak broadening and the clear emergence of the monoclinic  
35 signature. Rietveld refinements were done to evaluate the average crystallite size and the phase  
36 composition of the samples. A significant increase in the nanoparticle size from 3.7 nm up to  
37 7.0 nm is observed when 20 vol.% is added in benzyl alcohol but the nanometric nature of the  
38 samples appears to be maintained despite the presence of water in the initial reaction mixture.  
39  
40  
41  
42  
43  
44  
45  
46  
47  
48  
49  
50  
51  
52  
53  
54  
55  
56  
57  
58  
59  
60

With regards to the respective fraction of each polymorph within the samples, the action of the  
added water into the initial reaction mixture and in particular the influence of its content seem  
to be a more modest factor than that of the concentration of alkoxide seen previously in the  
section III.1.a). Indeed, the phase distribution is not greatly disturbed and the proportion of m-  
ZrO<sub>2</sub> nanocrystals increases from 44% to 51% when 5 vol.% water is added, then reaches 59%

with a water addition of 10 vol.%, and no longer evolve in the case of a water addition of 20 vol.%. The applied parameters do not permit a full production of m-ZrO<sub>2</sub> nanocrystals. In the work of De Keukeleere *et al.*, in which the syntheses were performed with an extremely short reaction time and a low concentration of 0.13 mol.L<sup>-1</sup> for zirconium isopropoxide, no drastic change into the crystal phase was noticed for a water volume ratio of 11 vol.%.<sup>35</sup> Nevertheless, we can distinguish in their diagram the raise of a minor impurity corresponding to m-ZrO<sub>2</sub>, especially at 24-24.5° and at 28° at the bottom of the main broad peak of c-ZrO<sub>2</sub>. We have to note that the use of a low concentrated mixture and a short reaction time which reduces *de facto* the *in-situ* ageing time of the nanoparticles in the presence of water could be the reason why the crystal change is not enough noticeable in their case.



1  
2  
3 **Figure.3.** X-ray diffraction patterns of ZrO<sub>2</sub> nanoparticles prepared by the Na-free benzyl  
4 alcohol sol-gel route in the presence of deionized water, *i.e.* anhydrous (a), 5 vol.% (b), 10  
5 vol.% (c) and 20 vol.% (d) . Also shown are the estimated size and t-ZrO<sub>2</sub> weight fraction  
6 (inset).  
7  
8  
9

10 The initial presence of water into the reaction mixture essentially induces a growth of the  
11 nanoparticles and affects to a lesser extent the polymorphic distribution of the sample showing  
12 that the hydrolytic sol-gel reactions are activated and able to absorb a certain hydration of the  
13 medium. It is not possible to conclude precisely on the effect of the presence of water during  
14 the synthesis and especially the formation of the nanocrystals because the metal precursor  
15 modification toward inorganic clusters, the nucleation of the oxidic material, the particle growth  
16 and finally the ageing of the particles are not distinguishable but overlapped steps. We can just  
17 underline that the presence of water by means of its ionizing, dispersing and solvating actions  
18 will drastically modify the surface chemistry of the particles.  
19  
20  
21  
22  
23  
24  
25  
26  
27  
28  
29

30 To assess the effect of a forced ageing in anhydrous or partially aqueous medium, as-  
31 synthesized wet particles were submitted to a subsequent solvothermal post-treatment for at  
32 least 48 hours at 210°C. The reaction medium of the second treatment consisted of either  
33 anhydrous benzyl alcohol or a mixture of benzyl alcohol and deionized water in volume ratios  
34 of 5, 20 and 50 vol.%. The resulting aged-powders were analyzed by XRD and the results are  
35 summarized in the Figure 4. The witness experiment obtained after a second treatment in  
36 anhydrous benzyl alcohol certifies that the anhydrous solvothermal post-treatment has only  
37 minor effect on the phase purity since the proportion of m-ZrO<sub>2</sub> nanocrystals is around 41 wt.%  
38 and almost the same than at the end of the initial solvothermal treatment. The particle size of  
39 the crystalline sample is evaluated at 3.7 nm and just reflects a small crystallite growth. Once  
40 water is added for the solvothermal post-treatment, the XRD diagrams show that the presence  
41 of water into the mixture plays a key role in the monoclinic content of the aged-particles. Indeed  
42 5 vol.% of water as co-solvent appears to be sufficient to modify the nature of the sample and  
43  
44  
45  
46  
47  
48  
49  
50  
51  
52  
53  
54  
55  
56  
57  
58  
59  
60



thus to change the shape of the diffraction pattern including the shoulder evidenced at  $28^\circ$ . The proportion of m-ZrO<sub>2</sub> nanocrystals reaches almost 57 wt.%. When the water content reaches a value of 20 vol.% the sample appears to be largely consisting of crystalline nanoparticles of monoclinic variety; indeed, the proportion of m-ZrO<sub>2</sub> nanocrystals is around 84 wt.%. Post-treatment in the presence of a large quantity of water (50 vol.%) does not change the particle size of the monoclinic phase neither the purity of the phase since the proportion of m-ZrO<sub>2</sub> nanocrystals is around 89 wt.% probably due to the fact that water and benzyl alcohol are only partially miscible even at 210°C and this limits the hydrolysis of the organophilic particles.

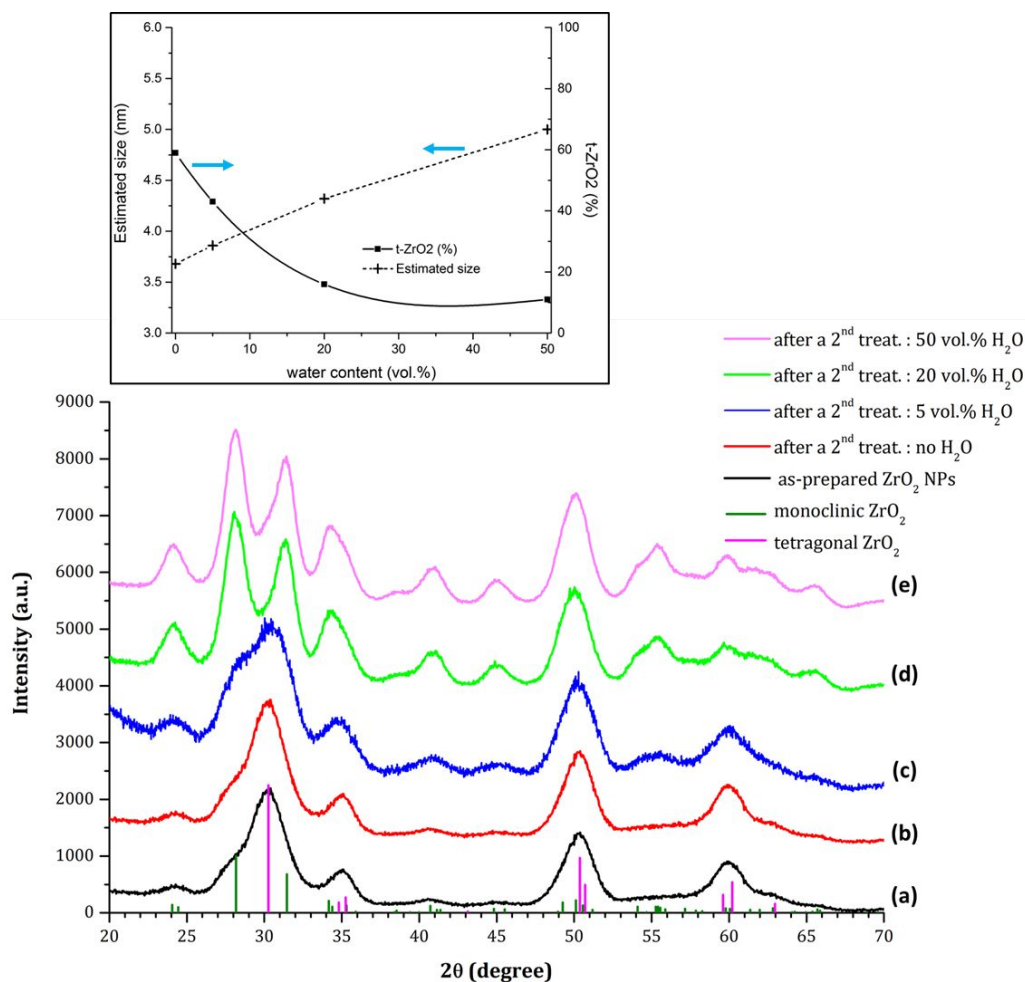


**Figure.4.** X-ray diffraction patterns of ZrO<sub>2</sub> nanoparticles after a solvothermal post-treatment in a mixture of benzyl alcohol and deionized water with volume ratios of 0, 5, 20 and 50 vol.% (a-e). Also shown are the estimated size and t-ZrO<sub>2</sub> weight fraction (inset).

1  
2  
3  
4  
5  
6 Those results, *i.e.* the effect of the presence of water in the initial reaction mixture and/or  
7 effect of a subsequent solvothermal post-treatment in hydrated medium, suggest that the  
8 biphasic nature of the reference sample synthesized in anhydrous benzyl alcohol with a nominal  
9 zirconium isopropoxide concentration of 0.32 mol.L<sup>-1</sup> is essentially due to the side dehydration  
10 reaction of isopropanol and to the release of water during the solvothermal treatment. We  
11 evidenced a water-induced phase conversion of the t-ZrO<sub>2</sub> into m-ZrO<sub>2</sub> nanoparticles which  
12 overpasses the stabilization offered by the critical size effect evidenced by Garvie. Xie *et al.*  
13 found that pure t-ZrO<sub>2</sub> nanocrystals exhibiting large surface area underwent a tetragonal-to-  
14 monoclinic transformation of about 78% after 12 hours of immersion in liquid water or aqueous  
15 vapor at 25°C.<sup>8</sup> Moreover, the transformation was not accompanied by any particle growth or  
16 surface area change. From these observations, they attributed the origin of this polymorphic  
17 transformation to a decrease in the driving force initially responsible for the room temperature  
18 stabilization of t-ZrO<sub>2</sub>. They concluded that under water exposure, the hydration of the  
19 nanoparticle surface leads to a significant decrease of the difference in surface free energy  
20 between the two polymorphs and thus to a strong decrease of the critical size.

21  
22  
23  
24  
25  
26  
27  
28  
29  
30  
31  
32  
33  
34  
35  
36  
37  
38  
39  
40 Such a transformation was probably not detected by Garnweitner *et al.* and De Keukeleere *et*  
41 *al.* because they synthesized their samples at lower zirconium precursor concentrations than  
42 those selected in this study and especially for De Keukeleere *et al.* with a fast and effective  
43 microwave solvothermal treatment.<sup>25,35,38</sup> We can conclude that the water-induced phase  
44 conversion is clearly dependent on the water content of the reaction mixture but also on the  
45 reaction time of the solvothermal treatment since some organic ligands cover the nanoparticles  
46 surface and slow down the process. The largest fraction of m-ZrO<sub>2</sub> nanoparticles evidenced in  
47 the sample prepared with the highest zirconium alkoxide concentration of 1.28 mol.L<sup>-1</sup> could  
48 be explained by: (i) the formation of a large number of nanoparticles per volume unit, (ii) the  
49  
50  
51  
52  
53  
54  
55  
56  
57  
58  
59  
60

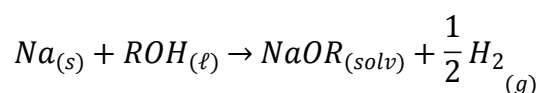
1  
2  
3 development of a large surface capable of catalyzing isopropanol dehydration, (iii) the release  
4 of a large content of water and thus, (iv) the extensive tetragonal-to-monoclinic transformation  
5  
6 induced by the highest water content.  
7  
8

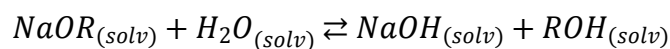
9  
10 It is well known to date that depending on its crystalline polymorphs, zirconia can be used in  
11 numerous applications like oxygen sensors, gate dielectrics and bioactive coatings. For  
12 example, the catalytic conversion of syngas will lead either to ethanol or to isobutanol  
13 depending on whether they are tetragonal or monoclinic polymorphs. It is therefore crucial to  
14 be able to obtain single phase and crystalline nanoparticles. Whereas De Keukeleere and  
15 coworkers have developed a fast and tunable synthesis of ZrO<sub>2</sub> nanocrystals limiting the  
16 eventuality of water-induced phase conversion, we propose another strategy which enables the  
17 production of pure t-ZrO<sub>2</sub> nanoparticles whatever the precursor and its concentration selected  
18 for the synthesis.  
19  
20  
21  
22  
23  
24  
25  
26  
27  
28  
29  
30  
31  
32

### 33 **III.2. Water-free production of t-ZrO<sub>2</sub> nanocrystals**

34  
35

36 In order to avoid the detrimental effect of water on the phase purity of nanocrystals  
37 synthesized by the benzyl alcohol route, we decided to introduce a sodium source in the form  
38 of sodium metal. Indeed, it was found in the literature that alkali cations covering zirconia  
39 catalyst are susceptible to inhibit zirconia-catalyzed alcohol dehydration.<sup>42</sup> Moreover, sodium  
40 alkoxides issued from the dissolution of sodium metal are able to neutralize traces of water and  
41 give another chance to limit and to trap any water molecules that may appear during the  
42 synthesis. This method firstly proposed by Kyrides *et al.* has proven to be a suitable procedure  
43 for dehydration of an alcoholic medium.<sup>43</sup> The reactions occurring during the process are  
44 represented as follows:  
45  
46  
47  
48  
49  
50  
51  
52  
53  
54  
55





The experimental protocol was simply modified by including a preliminary step of sodium metal dissolution in benzyl alcohol at room temperature for at least 30 minutes. This transparent sodium benzoxide solution is then used for the rest of the synthesis conformingly to the protocol exposed in the experimental section.

### a) Effect of sodium-to-zirconium molar ration on sample purity

In this part, the influence of the nominal sodium content used to generate the sodium benzoxide species is first studied in the case of a zirconium isopropoxide concentration of 0.32 mol.L<sup>-1</sup> and then developed for extremely high zirconium isopropoxide concentration of 1.28 mol.L<sup>-1</sup> in order to illustrate the exceptional efficiency of the proposed method.

In the case of a zirconium isopropoxide concentration of 0.32 mol.L<sup>-1</sup>, we found a strong dependence of the sample purity by varying the content of sodium metal from 0, 0.05, 0.10, 0.20, 0.40 and 1.0 mol.L<sup>-1</sup> as it is shown in the Figure 5. Up to a concentration of 0.10 mol.L<sup>-1</sup> in sodium, the presence of m-ZrO<sub>2</sub> polymorph is still discernable but tends to vanish since the fraction of m-ZrO<sub>2</sub> decreases from 44 wt.% to 40 wt.% for a sodium concentration of 0.05 mol.L<sup>-1</sup> and to 23 wt.% for a sodium concentration of 0.10 mol.L<sup>-1</sup>. From 0.20 to 0.40 mol.L<sup>-1</sup>, the final sample is only characterized by the presence of the t-ZrO<sub>2</sub> phase while a secondary phase appears for a high molar ratio in sodium of 1.0 mol.L<sup>-1</sup>. It is important to indicate that the content of sodium benzoxide species strongly impacts the purity of the final zirconia sample but also promotes the crystalline growth. Indeed, the particle size is 3.2 nm for a sodium concentration of 0.20 mol.L<sup>-1</sup> and reaches 4.8 nm when a sodium concentration of 0.40 mol.L<sup>-1</sup> is applied. At last, an excessive addition of sodium causes the appearance of an extra compound attributed to sodium zirconate, Na<sub>2</sub>ZrO<sub>3</sub> jointly to the narrowing of the Bragg

reflections of the zirconia nanoparticles indicating that the reaction mixture and especially the by-products have an activated action on the particle growth.

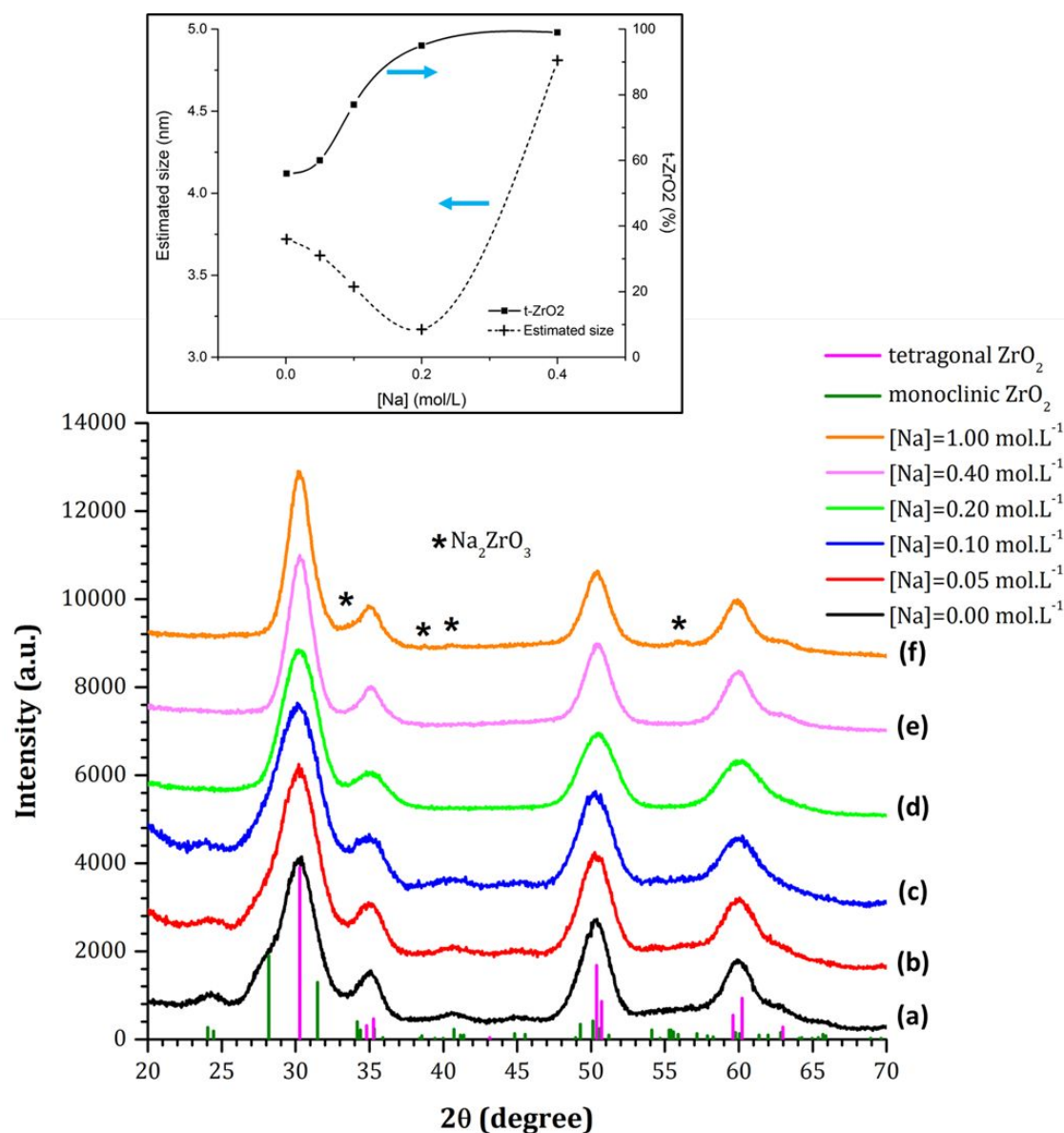


**Figure.5.** X-ray diffraction patterns of ZrO<sub>2</sub> nanoparticles prepared with [Zr]=0.32 mol.L<sup>-1</sup> by the Na-based benzyl alcohol sol-gel route as a function of the Na content (mol.L<sup>-1</sup>) in the reaction mixture. The stars underline the characteristic peaks of Na<sub>2</sub>ZrO<sub>3</sub> signature. Also shown are the estimated size and t-ZrO<sub>2</sub> weight fraction (inset).

From 0.10 up to 0.40 mol.L<sup>-1</sup>, the samples are single phased and one can observe together with the disappearance of the monoclinic polymorph a slight decrease in the peak broadening of t-ZrO<sub>2</sub> indicating that the best compromise between the polymorphic selection and the grain

1  
2  
3 growth limitation seems to be a concentration of 0.20 mol.L<sup>-1</sup> in sodium metal for a zirconium  
4 isopropoxide concentration of 0.32 mol.L<sup>-1</sup>. For this sample, the Rietveld refinement of the  
5 XRD diagram using the tetragonal symmetry gives an apparent size of 3.51 nm.  
6  
7

8  
9  
10 Another series of experiments was conducted in order to confirm the efficiency of the  
11 proposed experimental strategy to promote a good phase purity whatever the precursor content.  
12 The concentration in zirconium isopropoxide was increased by a factor 4 up to 1.28 mol.L<sup>-1</sup>  
13 with two different concentrations of sodium metal of 0.20 mol.L<sup>-1</sup> and 0.80 mol.L<sup>-1</sup>  
14 corresponding to a sodium-to-zirconium molar ratio of around 0.15 and 0.62 respectively. The  
15 molar ratio of 0.62 corresponds to the sodium-to-zirconium ratio used in the case of the  
16 optimized sample prepared with zirconium isopropoxide at 0.32 mol.L<sup>-1</sup> and sodium metal at  
17 0.20 mol.L<sup>-1</sup> whereas the molar ratio of 0.15 corresponds to the sodium-to-zirconium ratio used  
18 in the case of the sample prepared with zirconium isopropoxide at 0.32 mol.L<sup>-1</sup> and sodium  
19 metal at 0.05 mol.L<sup>-1</sup>.  
20  
21  
22  
23  
24  
25  
26  
27  
28  
29  
30  
31  
32

33 The XRD diagrams of the resulting powders are gathered in the Figure 6. At first sight, the  
34 content of monoclinic phase seems to be dependent on the concentration of zirconium alkoxide  
35 and then on the concentration of isopropanol that can be released upon the dissolution of the  
36 precursor and the ligand exchange reaction. In the absence of alkaline species, a larger  
37 concentration of the isopropanol adduct leads to a larger content of monoclinic nanocrystals  
38 which confirms that the isopropanol dehydration is the predominant side-reaction responsible  
39 for the proportional phase conversion process. At high concentration in zirconium alkoxide, it  
40 is not possible to recover a single-phase sample by the use of sodium in 0.20 mol.L<sup>-1</sup>  
41 concentration as it was the case for the optimized Na-based t-ZrO<sub>2</sub> sample but the Figure 6  
42 shows that the recovering of pure t-ZrO<sub>2</sub> nanocrystals is possible by using a larger concentration  
43 of sodium of 0.80 mol.L<sup>-1</sup>. Such a concentration corresponds to a sodium-to-zirconium molar  
44 ratio of 0.62, similar to those that has been used in the optimized conditions for the Na-based  
45  
46  
47  
48  
49  
50  
51  
52  
53  
54  
55  
56  
57  
58  
59  
60

benzyl alcohol route, and shows that a minimal sodium-to-zirconium molar ratio comprised between 0.31 and 0.62 is necessary to counterbalance the effect of the release of *in-situ* water.

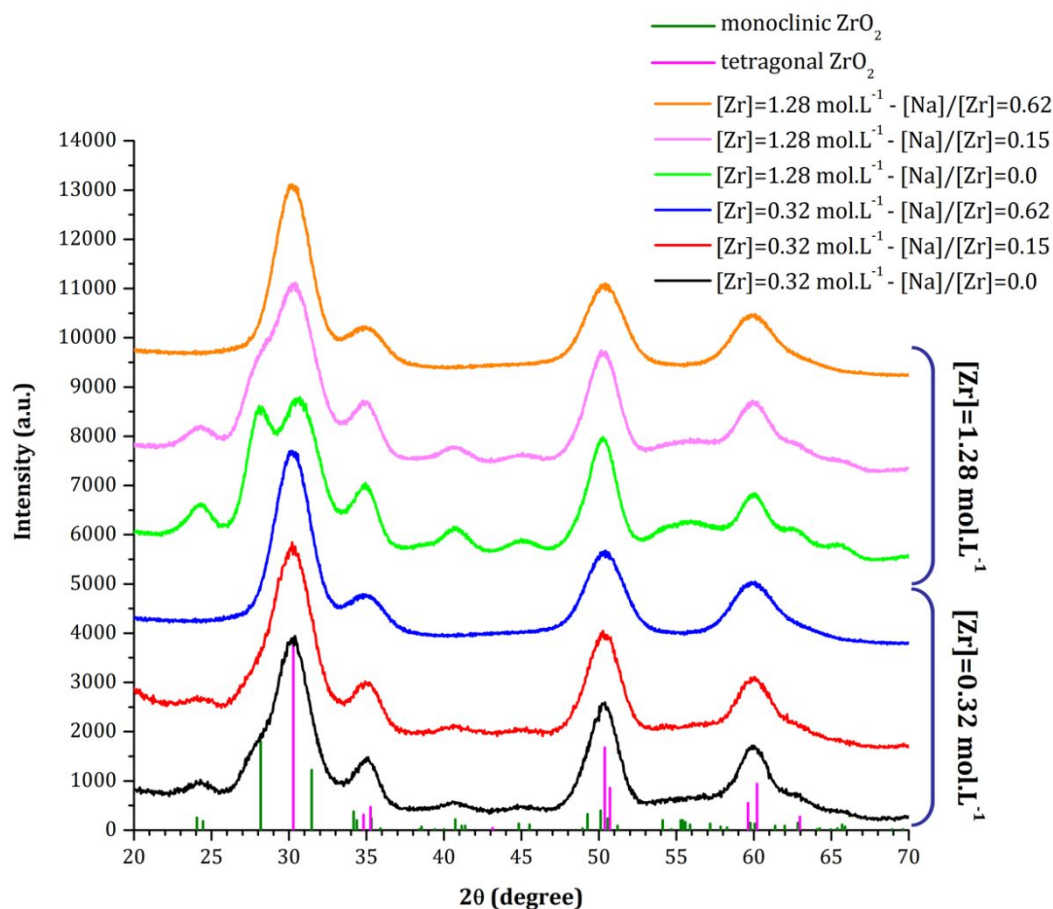


**Figure.6.** X-ray diffraction patterns of  $\text{ZrO}_2$  nanoparticles prepared by the benzyl alcohol route for two zirconium isopropoxide concentrations ( $0.32$  or  $1.28 \text{ mol.L}^{-1}$ ) w/out sodium introduced at a  $[\text{Na}]/[\text{Zr}]$  ratio of  $0$ ,  $0.15$  or  $0.62$ .

The crystallinity and morphology of the selected Na-based sample ( $[\text{Zr}]=0.32 \text{ mol.L}^{-1}$  and  $[\text{Na}]=0.20 \text{ mol.L}^{-1}$ ) were also confirmed by the TEM study displayed in the Figure 7. In the case of the washed and wet particles (Figure 7(a)), an overview image of the dispersion of nanoparticles on the TEM grid at low magnification illustrates that the sample prepared from the wet particles entirely consists of nanosized and monodisperse objects whereas the SAED analysis of the Figure 7(b) reveals some continuous and slightly diffuse diffraction rings corresponding to the tetragonal or cubic polymorph of zirconia. The last two images (Figure

7(c-d)) illustrate the isolated nature of the crystallized nanoparticles measuring around 3.0 nm whatever the way of TEM grid preparation by a wet or a dry process. The particles exhibit generally a more pronounced faceted-shape than the particles issued from the Na-free benzyl alcohol route. The alkaline medium and/or a possible change in the reaction pathway could be evocated in order to explain the more pronounced expression of crystallinity and the tailoring of faceted nanocrystals. Alkaline organic base or resulting hydroxide species after neutralization of water play a role of mineralizing agent favoring the solubility of surface ions imperfectly placed in the network and resulting in the exchange of these ions by others in order to achieve a crystal that would be gradually perfect.

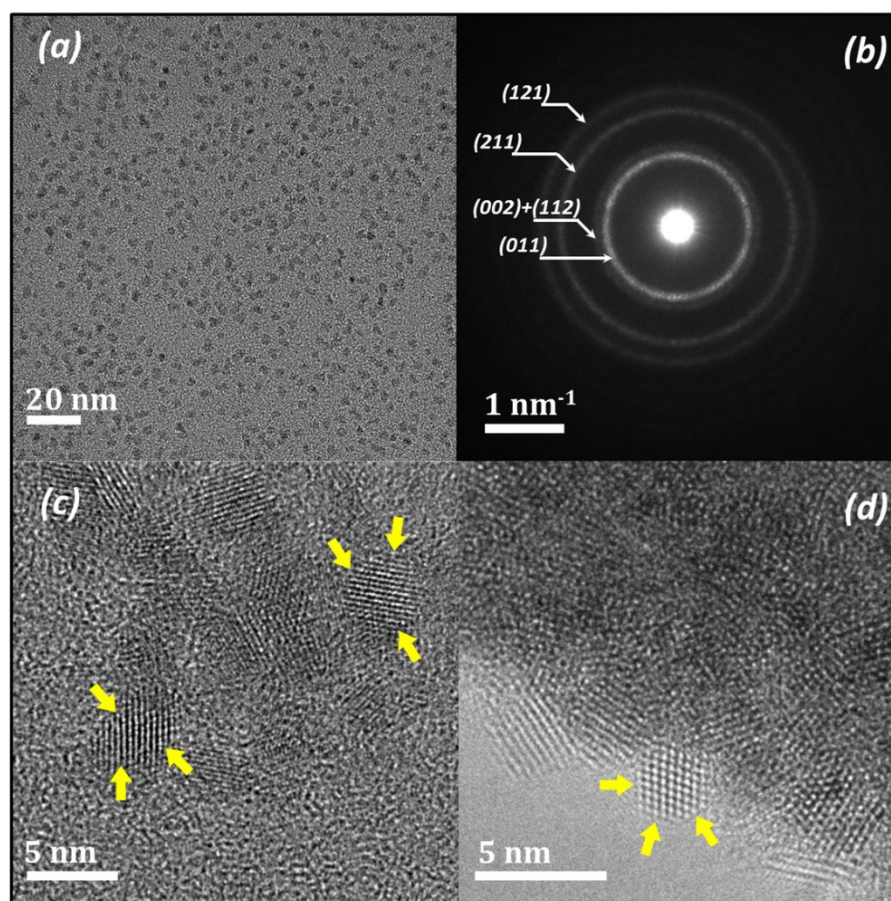


**Figure 7.** TEM micrographs of  $\text{ZrO}_2$  nanoparticles prepared by the Na-based benzyl alcohol route ( $[\text{Zr}] = 0.32 \text{ mol.L}^{-1}$  and  $[\text{Na}] = 0.20 \text{ mol.L}^{-1}$ ): (a) image of wet particles at low magnification, (b) diffraction rings of the corresponding wet particles, (c) and (d) images of dried particles.



1  
2  
3 According to the literature, under alkaline reaction conditions or in some rare cases in the  
4 presence of metal precursors exhibiting a strong Lewis acidity, the reaction between metal  
5 alkoxides and alcohols undergoes a Guerbet-type C-C coupling rather than an ether  
6 elimination.<sup>34,36-37,42</sup> To investigate a possible change in the condensation reaction, the  
7 supernatant liquid collected after centrifugation was subjected to <sup>13</sup>C and <sup>1</sup>H NMR analyses  
8 revealing the presence of the initial benzyl alcohol, isopropanol, minor presence of  
9 4-phenyl-2-butanol ( $\beta$ -ramified Guerbet alcohol) and the absence of water (Figure.S2. in  
10 supporting information).  
11  
12  
13  
14  
15  
16  
17  
18  
19  
20

21 Since only minor quantity of 4-phenyl-2-butanol is found into the supernatant, the mechanism  
22 for the formation of M-O-M network is thus possibly based on C-C coupling and/or a direct  
23 hydroxylation of the metal alkoxide by NaOH which is a byproduct of the neutralization of  
24 water by sodium benzoate.<sup>38</sup> The Guerbet mechanism occurs *via* a complex sequence in  
25 several steps; namely, (i) dehydrogenation or oxidation of the alcohol to aldehyde, (ii) aldol  
26 condensation of aldehyde and enolate, (iii) dehydration of the aldol product, and, finally (iv)  
27 hydrogenation of the  $\alpha,\beta$ -unsaturated ketone giving the Guerbet alcohol. According to the work  
28 of Kozlowski, even if the alkali metal activates slightly the dehydrogenation reaction of alcohol,  
29 sodium cations tend to disrupt the appropriate acid-base pairs on the surface of zirconia, inhibit  
30 the aldol condensation step and then limit the possibility for the chemical system to generate  
31 Guerbet alcohols.<sup>42</sup>  
32  
33  
34  
35  
36  
37  
38  
39  
40  
41  
42  
43  
44  
45

46 Finally, the addition of sodium metal to the benzyl alcohol at a concentration of 0.20 mol.L<sup>-1</sup>  
47 succeeded for a zirconium isopropoxide concentration of 0.32 mol.L<sup>-1</sup> to eliminate the traces of  
48 water. Concerning the absence of water into the supernatant, two hypotheses or a combination  
49 of both can be proposed: either based on the proposition of Kyrides the acid-base neutralization  
50 of water occurs owing to the sodium benzoate species and/or as it was proposed by Kozlowski  
51  
52  
53  
54  
55  
56  
57  
58  
59  
60

1  
2  
3 the inhibition of isopropanol dehydration onto zirconia nanoparticles is due to Na<sup>+</sup> pollution all  
4 over the surface.<sup>42-43</sup>  
5  
6  
7  
8  
9

## 10 **b) Complementary experiments: localization of Na**

11  
12  
13  
14 To investigate how the modification of the benzyl alcohol route by the addition of sodium  
15 metal is acting and what specificities have to be taken in account, we have performed  
16 complementary experiments, namely ICP-AES, thermal analyses, and, FTIR spectroscopy.  
17  
18  
19

20  
21 According to the ICP-AES measurements, a weight fraction of approximately 0.08 in sodium  
22 has been measured in the sample prepared with the following conditions [Zr]=0.32 mol.L<sup>-1</sup> and  
23 [Na]=0.20 mol.L<sup>-1</sup>. Although the weight fraction value is quite large, it could be explained by  
24 taking into account the large developed specific surface commonly found in the case of  
25 nanoparticles compared to those observed for larger micrometric systems. Even if the cations  
26 are supposed to be used for the surface covering of the particles, it is not excluded that a  
27 Na<sup>+</sup>-doping phenomenon occurs and stabilizes the t-ZrO<sub>2</sub> phase. For both cases, Na-free or Na-  
28 modified benzyl alcohol route, powders were submitted to thermal gravimetric analyses.  
29  
30 Displayed in the Figure 8 the thermal gravimetric curves exhibit the same global feature  
31 composed of two main weight losses. The first weight loss is generally attributed to the  
32 evaporation of solvents and physically adsorbed molecules. From room temperature to 400°C,  
33 the weight loss is of about 8.4% for the sodium-free sample and 10.2% for the sodium-based  
34 sample. The second weight loss is detectable around 440°C for the sodium-free sample and  
35 estimated to 5.5%; such feature is usually attributed to the release of chemisorbed molecules,  
36 to the dehydration of hydroxyl and alkoxy groups and of course to the combustion of residual  
37 organics. In the case of the sodium-based synthesis, the second weight loss is shifted up to  
38 650°C and supposed to correspond to the decarbonation of a refractory intermediate compound,  
39  
40  
41  
42  
43  
44  
45  
46  
47  
48  
49  
50  
51  
52  
53  
54  
55  
56  
57  
58  
59  
60

possibly  $\text{Na}_2\text{CO}_3$  which shall decompose at higher temperature around  $650^\circ\text{C}$ - $750^\circ\text{C}$ . The formation of sodium carbonate could occur at the surface of the nanoparticles due to air exposure at the end of the drying step, after the full removal of dichloromethane, followed by the acid-base reaction of carbon dioxide onto the surface of the particles. In order to support this hypothesis, FTIR analysis has been undertaken and the presence of carboxylate or carbonate species was evidenced in the dried powder. Indeed, the FTIR spectrum of the modified Na-based benzyl alcohol route exhibits two bands at  $1550\text{ cm}^{-1}$  and  $1430\text{ cm}^{-1}$  that can be attributed to the vibrational band of the carbonyl function of a carboxylate or carbonate group (Figure.S3. in supporting information).

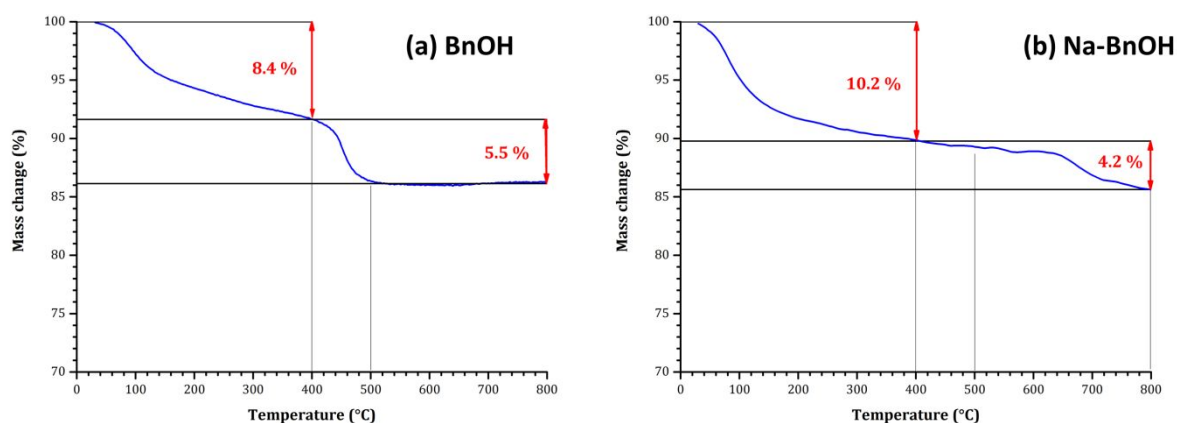
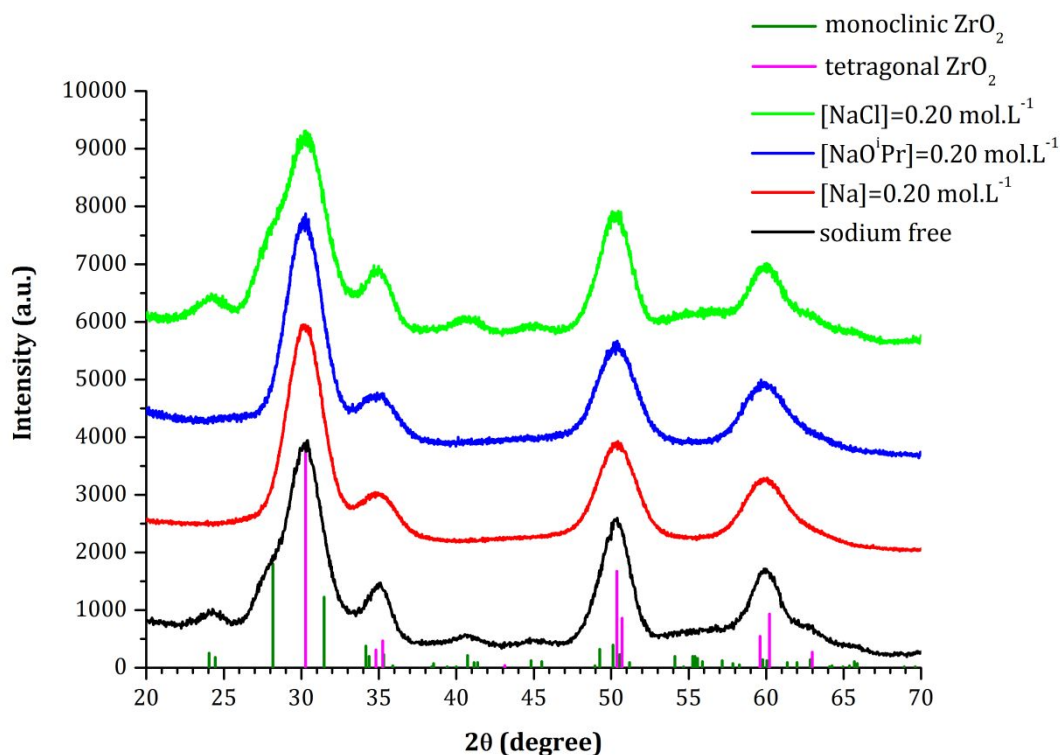


**Figure.8.** TG curves of  $\text{ZrO}_2$  nanoparticles obtained (a) by a Na-free procedure and (b) by a Na-based procedure in air ( $10^\circ\text{C}\cdot\text{min}^{-1}$ ).

Even if the results indicate that the largest part of the sodium is located at the surface of the nanoparticles where it forms a carbonate compound, a possible  $\text{Na}^+$ -doping phenomenon is not discarded. To highlight this questionable aspect we examine if the use of different sodium sources for the Na-modified benzyl alcohol route leads also to the stabilization of t- $\text{ZrO}_2$  nanoparticles. The last series of syntheses consisted to use and to compare the effect of different sodium sources, *i.e.* sodium metal (Na), sodium isopropoxide ( $\text{NaO}^i\text{Pr}$ ) and lastly sodium chloride (NaCl) maintaining all the other parameters ( $210^\circ\text{C}$ , 48 hours and  $[\text{Zr}]=0.32\text{ mol}\cdot\text{L}^{-1}$

1  
2  
3 and  $[\text{Na source}] = 0.20 \text{ mol.L}^{-1}$ ). It is important to note that whereas sodium benzoate or  
4 isopropoxide are some strong organic bases in nonaqueous amphiprotic medium like alcohols,  
5 chloride only expresses a weak Brønsted and borderline Lewis basicities. The XRD diagrams  
6 of the resulting samples are gathered in the Figure 9. By comparison with the Na-free sample,  
7 the Na- and the  $\text{NaO}^i\text{Pr}$ -based samples are exclusively composed of pure t- $\text{ZrO}_2$  nanoparticles  
8 whereas the NaCl-based sample remains definitively biphasic in nature. This last result  
9 demonstrates that the presence of  $\text{Na}^+$  is not a sufficient factor to suppress the phase conversion  
10 of t- $\text{ZrO}_2$  into m- $\text{ZrO}_2$  phase contrary to what was observed in the Na-based- or  $\text{NaO}^i\text{Pr}$ -based  
11 benzyl alcohol syntheses.  
12  
13  
14  
15  
16  
17  
18  
19  
20  
21  
22  
23



49 **Figure.9.** X-ray diffraction patterns of  $\text{ZrO}_2$  nanoparticles prepared by the benzyl alcohol route  
50 w/out sodium-based reactant ( $\text{Na}$ ,  $\text{NaO}^i\text{Pr}$  or  $\text{NaCl}$ ) introduced at  $0.2 \text{ mol.L}^{-1}$ .  
51  
52

53 It gives also an indirect evidence that the phase selection mechanism does not operate *via* a  
54  $\text{Na}^+$ -doping effect but much more likely *via* a complex interplay of at least two main factors,  
55  
56  
57  
58  
59  
60

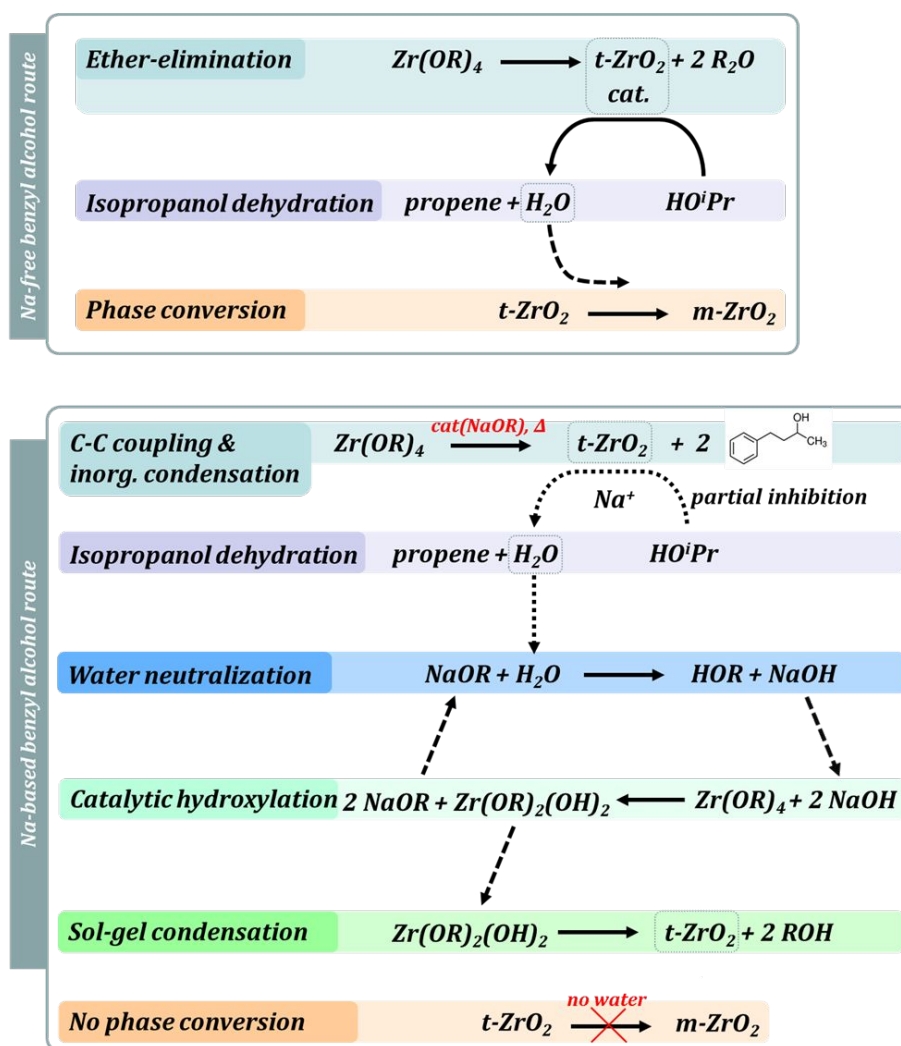
1  
2  
3 *i.e.* the strong alkalinity of the anionic species appearing during the process and in a lesser  
4 extent the cationic capping of the nanoparticle surface inducing acid-base sites disruption.  
5  
6  
7  
8  
9

### 10 **III.3. Discussion**

11  
12  
13 While the standard benzyl alcohol route of zirconium isopropoxide-isopropanol adduct based  
14 on an ether-elimination reaction leads to a biphasic mixture, the dissolution of sodium metal  
15 into anhydrous benzyl alcohol prior to the solvothermal treatment definitively plays a role of  
16 primary importance in order to obtain single-phase tetragonal nanocrystals. One important fact  
17 is that there was no difference in the average size estimated by Rietveld refinement or by TEM  
18 observation between both *t*- and *m*-ZrO<sub>2</sub> nanocrystals which means that no size effect seems to  
19 govern the polymorph conversion and the synthesis of a biphasic sample.  
20  
21  
22  
23  
24  
25  
26  
27  
28

29 The progressive disappearance of the monoclinic contribution into the samples was observed  
30 as to follow that of the increase in the sodium metal content or more precisely the increase in  
31 the sodium benzoxide content. Beyond a certain amount comprised between the molar  
32 concentrations of 0.10 and 0.20 mol.L<sup>-1</sup> in sodium benzoxide, the content is large enough to  
33 neutralize the water appearing during the solvothermal treatment or to simply inhibit NP  
34 surface-catalyzed alcohol dehydration. The range of concentration corresponds to a sodium-to-  
35 zirconium molar ratio between 0.31 and 0.62 with which the final mixture is found to be  
36 exclusively composed by some single-phase *t*-ZrO<sub>2</sub> nanocrystals without any excessive particle  
37 growth.  
38  
39  
40  
41  
42  
43  
44  
45  
46  
47  
48

49 Two synthesis schemes for both benzyl alcohol and sodium-modified benzyl alcohol routes  
50 are proposed in the Figure 10.  
51  
52  
53  
54  
55  
56  
57  
58  
59  
60



37 **Figure.10.** Summary of the main reactions involved in the Na-free and Na-based benzyl alcohol  
38 routes.

41 The emergence of the  $m-ZrO_2$  nanocrystals in the case of the synthesis without or with only  
42 a low sodium content was attributed to the detrimental presence of *in-situ* water issued from a  
43 side-reaction as it is summarized in the top of the Figure 10. Such water is presumably released  
44 from a surface-mediated dehydration mechanism of the alcoholic medium due to the  
45 amphoteric, and especially acidic, properties of zirconia nanocrystals. More precisely, the  
46 correlation between the  $m-ZrO_2$  content and the concentration of the zirconium isopropoxide-  
47 isopropanol adduct let us to think that the dehydration reaction essentially concerns the  
48 isopropanol molecules coming from the zirconium precursor or issued from the alcohol  
49  
50  
51  
52  
53  
54  
55  
56  
57  
58  
59  
60

1  
2  
3 exchange reaction with benzyl alcohol and leads to the release of volatile propene and water.  
4  
5 The intentional addition of water into the reaction vessel as well as a post-synthesis retreatment  
6  
7 of the freshly as-prepared particles in the presence of water has shown that the water degraded  
8  
9 the purity of the samples and induced an effective phase conversion process proportional to the  
10  
11 water content introduced into the reactor. Such observations have already been reported by  
12  
13 Murase *et al.* who evidenced the transformation of metastable tetragonal zirconia into  
14  
15 monoclinic one upon thermal treatment or contact with water vapor at 400°C.<sup>12</sup> Xie *et al.*  
16  
17 confirmed the same feature by *in situ* Raman spectroscopy in the case of calcined zirconium  
18  
19 oxyhydroxide which leads to tetragonal zirconia upon heat-treatment at 350°C and then  
20  
21 transforms into monoclinic zirconia without any drastic loss in surface area by the simple  
22  
23 exposure to water vapor even at room temperature.<sup>8</sup> Since the tetragonal-to-monoclinic  
24  
25 transformation is described as a martensitic and diffusion-less process, there is no activation  
26  
27 barrier for the process to occur and the only limitation lies in the formation of nucleation sites.  
28  
29 We presume that such sites nucleate once the nanoparticles surface is depassivated, which  
30  
31 means extensively hydrolyzed to remove organic ligands. The initiation of the water-induced  
32  
33 phase conversion could be similar to the low thermal degradation observed for micrometric  
34  
35 zirconia but is still unclear.<sup>44</sup>  
36  
37  
38  
39  
40  
41

42 The role played by the sodium alkoxide during the particle formation and the ageing of the  
43  
44 suspension was ascertained by the substitution of Na metal with NaO<sup>i</sup>Pr and NaCl (even sodium  
45  
46 hydroxide can be used but the result is not shown here). Taking in account that the Na<sup>+</sup> cations  
47  
48 covering the surface of the zirconia nanoparticles are only partially inhibiting the dehydration  
49  
50 side-reaction, we suggest that the strong alkalinity of the reaction mixture enables the sol-gel  
51  
52 process to pursue in a non-hydrolytic manner. In the bottom of the Figure 10, we propose a  
53  
54 summary of the different roles of sodium alkoxide. First, sodium alkoxide is a prerequisite for  
55  
56 the C-C bond formation, the hydroxylation of the zirconium precursor and further the  
57  
58  
59  
60

1  
2  
3 condensation into  $\text{ZrO}_2$  nanoparticles. Such reaction is validated but only in a limited extent.  
4  
5 Indeed,  $\text{Na}^+$  is known to partially inhibit the Guerbet-like mechanism which is corroborated by  
6  
7 the minor presence of 4-phenyl-2-butanol at the end of the solvothermal treatment. Secondly,  
8  
9 the presence of  $\text{Na}^+$  is also known to decrease the catalytic activity of the NP surface toward  
10  
11 alcohol dehydration by poisoning its surface. Anyway sodium alkoxide can neutralize traces of  
12  
13 water and releases sodium hydroxide which, in turn, is able to promote the inorganic  
14  
15 condensation *via* a catalytic hydroxylation reaction. Following the non-hydrolytic  
16  
17 hydroxylation, sodium alkoxide is regenerated and the hydroxylated species can undergo  
18  
19 condensation *via* an alternate and/or complementary sol-gel reactions. At last, parallel to the  
20  
21 formation process, the absence of water prevents the t- $\text{ZrO}_2$  nanoparticles to convert into  
22  
23 monoclinic ones.  
24  
25  
26  
27

28  
29 Interestingly, it was shown that the Na-modified benzyl alcohol route gave excellent results  
30  
31 in terms of purity and limited particles size providing that the sodium-to-zirconium molar ratio  
32  
33 was adjusted to at least 0.62. The possibility to increase significantly the concentration of the  
34  
35 reactants is of crucial interest when the chemical process is based on expensive solvent or when  
36  
37 it is necessary to consider some industrial-scale or semi-industrial-scale developments.  
38  
39

40  
41 The surface of the nanoparticles would require further investigations in terms of properties  
42  
43 especially to determine the impact of the presence of sodium-based species poisoning the  
44  
45 surface.  
46  
47  
48

#### 49 **IV. CONCLUSION**

50

51  
52 In conclusion, the tremendous effect of the presence of water on the growth and  
53  
54 destabilization of t- $\text{ZrO}_2$  produced *via* the benzyl alcohol route was evidenced experimentally.  
55  
56 Such a water, either intentionally added in the reaction mixture or issued from the dehydration  
57  
58 of alcohol during a prolonged heat treatment (and specially a high zirconium alkoxide  
59  
60



1  
2  
3 concentration), was shown to play a detrimental role similar to what was observed in the low  
4 thermal degradation of bulk zirconia. In order to remedy the deterioration of the sample purity,  
5 we investigated the use of different sodium sources, namely sodium metal, sodium chloride or  
6 sodium isopropoxide, and found that the crystalline phase was affected if the sodium source  
7 was able to exhibit a strong basicity. Indeed, the Brønsted acid-base consumption of water by  
8 sodium alkoxide coupled with a Na<sup>+</sup> capping of the nanoparticle surface was found to be  
9 necessary to inhibit the isopropanol dehydration and/or to neutralize the *in-situ* water without  
10 promoting an excessive particle growth.  
11  
12  
13  
14  
15  
16  
17  
18  
19  
20

21 The addition of a basic salt has been found to be a suitable strategy able to avoid the loss of  
22 phase purity and to recover the phase stabilization of t-ZrO<sub>2</sub> nanoparticles offered by the critical  
23 size effect. This strategy was shown to be effective even when the dehydration side-reaction  
24 responsible for the release of water is promoted by a large increase of the alkoxide concentration  
25 and/or by a prolonged heat-treatment. Such a situation is generally encountered due to the  
26 reduction of the economic cost of a process, *i.e.* for example by decreasing the content of  
27 anhydrous benzyl alcohol and/or by choosing a less expensive zirconium alkoxide as zirconium  
28 n-propoxide even if the parent alcohol is quite more sensitive to dehydration upon prolonged  
29 solvothermal treatment than isopropanol itself.  
30  
31  
32  
33  
34  
35  
36  
37  
38  
39  
40  
41  
42  
43  
44

## 45 **ASSOCIATED CONTENT**

### 46 **Supporting Information**

47  
48  
49  
50  
51 NMR analyses of the sodium-free synthesis ([Zr]=0.32 mol.L<sup>-1</sup>, 210°C for 48 hours), NMR  
52 analyses of the sodium-based synthesis ([Zr]=0.32 mol.L<sup>-1</sup>, [Na]/[Zr]=0.62, 210°C for 48  
53 hours), FTIR analysis of the zirconia nanoparticles prepared by the sodium-modified benzyl  
54 alcohol route ([Zr]=0.32 mol.L<sup>-1</sup>, [Na]/[Zr]=0.62, 210°C for 48 hours).  
55  
56  
57  
58  
59  
60

## AUTHOR INFORMATION

### Corresponding Author

E-mail: [fabien.remondiere@unilim.fr](mailto:fabien.remondiere@unilim.fr)

### Present addresses

Jess Gambe: Department of Physics, College of Science and Mathematics, MSU-Iligan Institute of Technology, Iligan city, Philippines

## ACKNOWLEDGEMENTS

We would like to thank Pierre Carles for TEM observations, Julie Cornette for FTIR spectroscopy, Sandra Blanchet for ICP-AES analyses and Yves Champavier for NMR recording.

## ABBREVIATIONS

NPs, nanoparticles; HO<sup>i</sup>Pr, isopropanol; O<sup>i</sup>Pr, isopropoxide; BnOH, benzyl alcohol; NaOBn, sodium benzoxide.

## REFERENCES

- (1) Garvie, R. C.; Hanink, R. H. J.; Pascoe, R. T.; Ceramic steel?, *Nature*, **1975**, 258, 703-704.
- (2) Yan, R.; Ding, D.; Lin, B.; Liu, M.; Meng, G.; Liu, X.; Thin yttria-stabilized zirconia electrolyte and transition layers fabricated by particle suspension spray, *J. Power Sources*, **2007**, 164, 567-571.

- 1  
2  
3 (3) Murase, Y.; Kato, E.; Role of water vapor in crystallite growth and tetragonal-monoclinic phase  
4 transformation of ZrO<sub>2</sub>, *J. Am. Ceram. Soc.*, **1983**, *66*, 196-200.  
5  
6  
7 (4) Kohno, Y.; Tanaka, T.; Funabiki, T.; Yoshida, S.; Photoreduction of carbon dioxide with hydrogen over  
8 ZrO<sub>2</sub>, *Chem. Commun.*, **1997**, 841-842.  
9  
10  
11 (5) Sayama, K.; Arakawa, H.; Photocatalytic decomposition of water and photocatalytic reduction of carbon  
12 dioxide over zirconia catalyst, *J. Phys. Chem.*, **1993**, *97*, 531-533.  
13  
14  
15 (6) Ho, S.-M.; On the structural chemistry of zirconium oxide, *Mater. Sci. Eng.*, **1982**, *54*, 23-29.  
16  
17  
18 (7) Reidy, C.-J.; Fleming, T.-J.; Hampshire, S.; Towler, M.-R.; Comparison of microwave and conventionally  
19 sintered yttria-doped zirconia ceramics, *Int. J. Appl. Ceram. Technol.*, **2011**, *8*, 1475-1485.  
20  
21  
22 (8) Bellido, J.-D.-A.; De Souza, J.-E.; M'Peko, J.-C.; Assaf, E.-M.; Effect of adding CaO to ZrO<sub>2</sub> support on  
23 nickel catalyst activity in dry reforming of methane, *Appl. Catal. A.*, **2009**, *358*, 215-223.  
24  
25  
26 (9) Garvie, R. C.; The occurrence of metastable tetragonal zirconia as a crystallite size effect, *J. Phys. Chem.*,  
27 **1965**, *69*, 1238-1243.  
28  
29  
30 (10) Garvie, R. C.; Stabilization of the tetragonal structure in zirconia microcrystals, *J. Phys. Chem.*, **1978**, *82*,  
31 218-224.  
32  
33  
34 (11) Shukla, S.; Seal, S. J.; Thermodynamic tetragonal phase stability in sol-gel derived nanodomains of pure  
35 zirconia, *Phys. Chem. B*, **2004**, *108*, 3395-3399.  
36  
37  
38 (12) Xie, S.; Iglesia, E.; Bell, A. T.; Water-assisted tetragonal-to-monoclinic phase transformation of ZrO<sub>2</sub> at  
39 low temperatures, *Chem. Mater.*, **2000**, *12*(8), 2442-2447.  
40  
41  
42 (13) Becker, J.; Hald, P.; Bremholm, M.; Pedersen, J. S.; Chevallier, J.; Iversen, S. B.; Iversen, B. B.; Critical  
43 size of crystalline ZrO<sub>2</sub> nanoparticles synthesized in near- and supercritical water and supercritical isopropyl  
44 alcohol, *ACS Nano*, **2008**, *2*, 1058-1068.  
45  
46  
47 (14) Rong, Y.; Meng, Q.; Zhang, Y.; Hsu, T. Y.; Phase stability and its intrinsic conditions in nanocrystalline  
48 materials, *Mater. Sci. Eng., A*, **2006**, *438*, 414-419.  
49  
50  
51  
52  
53  
54  
55  
56  
57  
58  
59  
60

- 1  
2  
3 (15) Yamaguchi, T.; Sasaki, H.; Tanabe, K.; High selectivities of zirconium oxide catalyst for isomerization  
4 of 1-butene and dehydration of sec-butanol, *Chem. Lett.*, **1973**, 1017-1018.  
5  
6  
7  
8 (16) Davis, B. H.; Metal oxide analogue of metal alloy catalysts, *Appl. Surf. Sci.*, **1984**, *19*, 200-217.  
9  
10  
11 (17) Kozłowski, J. T.; Davis, R. J.; Sodium modification of zirconia catalysts for ethanol coupling to 1-butanol,  
12 *J. Energy. Chem.*, **2013**, *22*, 58-64.  
13  
14  
15 (18) Nakano, Y.; Yamaguchi, T.; Tanabe, K.; Hydrogenation of conjugated dienes over ZrO<sub>2</sub> by H<sub>2</sub> and  
16 cyclohexadiene, *J. Catal.*, **1983**, *80*, 307-314.  
17  
18  
19  
20 (19) Lei, T.; Xu, J. C.; Tang, Y.; Hua, W. M.; Gao, Z.; New solid superacid catalysts for n-butane  
21 isomerization:  $\gamma$ -Al<sub>2</sub>O<sub>3</sub> or SiO<sub>2</sub> supported sulfated zirconia, *Appl. Catal. A*, **2000**, *192*, 181-188.  
22  
23  
24 (20) Stichert, W.; Schüth, F.; Kuba, S; Knözinger, H.; Monoclinic and tetragonal high surface area sulfated  
25 zirconias in butane isomerization: CO adsorption and catalytic results, *J. Catal.*, **2001**, *198*, 277-285.  
26  
27  
28  
29 (21) Morterra, C.; Cerrato, G.; Pinna, F.; Signoretto, M.; Crystal phase, spectral features, and catalytic activity  
30 of sulfate-doped zirconia systems, *J. Catal.*, **1995**, *157*, 109-123.  
31  
32  
33  
34 (22) Zhao, N.; Pan, D.; Nie, W.; Ji, X.; Two-phase synthesis of shape-controlled colloidal zirconia nanocrystals  
35 and their characterization, *J. Am. Chem. Soc.*, **2006**, *128(31)*, 10118-10124.  
36  
37  
38  
39 (23) Joo, J.; Yu, T.; Kim, Y. W.; Park, H. M.; Wu, F.; Zhang, J. Z.; Hyeon, T.; Multigram scale synthesis and  
40 characterization of monodisperse tetragonal zirconia nanocrystals, *J. Am. Chem. Soc.*, **2003**, *125(21)*, 6553-6557.  
41  
42  
43 (24) Inoue, M.; Kominami, H.; Inui, T; Novel synthetic method for the catalytic use of thermally stable  
44 zirconia: thermal decomposition of zirconium alkoxides in organic media, *Appl. Catal. A*, **1993**, *97*, L25-L30.  
45  
46  
47 (25) Kongwudthiti, S.; Praserttham, P.; Silveston, P.; Inoue, M.; Influence of synthesis conditions on the  
48 preparation of zirconia powder by the glycothermal method, *Ceram. Int.*, **2003**, *29*, 807-814.  
49  
50  
51  
52 (26) Garnweitner, G.; Goldenberg, L. M.; Sakhno, O. V.; Antonietti, M.; Niederberger, M.; Stumpe, J.; Large-  
53 scale synthesis of organophilic zirconia nanoparticles and their application in organic-inorganic nanocomposites  
54 for efficient volume holography, *Small*, **2007**, *3(9)*, 1626-1632.  
55  
56  
57  
58  
59  
60

1  
2  
3 (27) Zhou, S.; Garnweitner, G.; Niederberger, M.; Antonietti, M.; Dispersion behavior of zirconia nanocrystals  
4 and their surface functionalization with vinyl group-containing ligands, *Langmuir*, **2007**, *23*(18), 9178-9187.

5  
6  
7 (28) Niederberger, M.; Garnweitner, G.; Organic reaction pathways in the nonaqueous synthesis of metal oxide  
8 nanoparticles, *Chem. Eur. J.*, **2006**, *12*, 7282-7302.

9  
10  
11 (29) Garnweitner, G.; Grote, C.; In situ investigation of molecular kinetics and particle formation of water-  
12 dispersible titania nanocrystals, *Phys. Chem. Chem. Phys.*, **2009**, *11*(9), 3767-3774.

13  
14  
15 (30) Zhang, L.; Garnweitner, G.; Djerdj, I.; Antonietti, M.; Niederberger, M.; Generalized nonaqueous sol-gel  
16 synthesis of different transition-metal niobate nanocrystals and analysis of the growth mechanism, *Chem. Asian*  
17 *J.*, **2008**, *3*(4), 746-752.

18  
19  
20 (31) De Roo, J.; De Keukeleere, K.; Feys, J.; Lommens, P.; Hens, Z.; Van Driessche, I.; Fast, microwave-  
21 assisted synthesis of monodisperse HfO<sub>2</sub> nanoparticles, *J. Nanoparticle Res.*, **2013**, *15*(7).

22  
23  
24 (32) De Roo, J.; Van Driessche, I.; Martins, J.C.; Hens, Z.; Colloidal metal oxide nanocrystal catalysis by  
25 sustained chemically driven ligand displacement, *Nat. Mater.*, **2016**, *15*(5), 517-521.

26  
27  
28 (33) Wang, J.; Cao, F.; Bian, Z.; Leung, M.K.H.; Li, H.; Ultrafine single-crystal TiOF<sub>2</sub> nanocubes with  
29 mesoporous structure, high activity and durability in visible light driven photocatalysis, *Nanoscale*, **2014**, *6*(2),  
30 897-902.

31  
32  
33 (34) Niederberger, M.; Pinna, N.; *Metal oxide nanoparticles in organic solvents*, **2009**, Springer-Verlag  
34 London.

35  
36  
37 (35) De Keukelere, K.; De Roo, J.; Lommens, P.; Martins, J.C.; Van Der Voort, P.; Van Driessche, I.; Fast  
38 and tunable synthesis of ZrO<sub>2</sub> nanocrystals: mechanistic insights into precursor dependence, *Inorg. Chem.*; **2015**,  
39 *54*, 3469-3476.

40  
41  
42 (36) Guerbet, M.; Action des alcools sur les dérivés sodés d'autres alcools, *Compt. Rend.*, **1902**, *135*, 172-175.

43  
44  
45 (37) Guerbet, M.; Sur trois alcools primaires nouveaux résultant de la condensation du benzylate de sodium  
46 avec les alcools propylique, butylique et isoamylique, *Compt. Rend.*, **1908**, *146*, 1405-1407.

1  
2  
3 (38) Garnweitner, G., *Nonaqueous synthesis of transition-metal oxide nanoparticles and their formation*  
4 *mechanism (PhD dissertation)*, **2005**, University of Potsdam.

6  
7  
8 (39) Kostestkyy, P.; Yu, J.; Gorte, R.J.; Mpourmpakis, G.; Structure-activity relationships on metal-oxides:  
9 Alcohol dehydration, *Cat. Sci. & Tech.* ; **2014**, *4(11)*, 3861-3869.

11  
12 (40) Aramendia, M.A. ; Boráu, V. ; Jiménez, C. ; Marinas, J.M. ; Porras, A. ; Urbano, F.J. ; Synthesis and  
13 characterization of ZrO<sub>2</sub> as an acid-base catalyst: dehydration-dehydrogenation of propan-2-ol, *J. Chem. Soc.,*  
14 *Faraday Trans.*, **1997**, *93(7)*, 1431-1438.

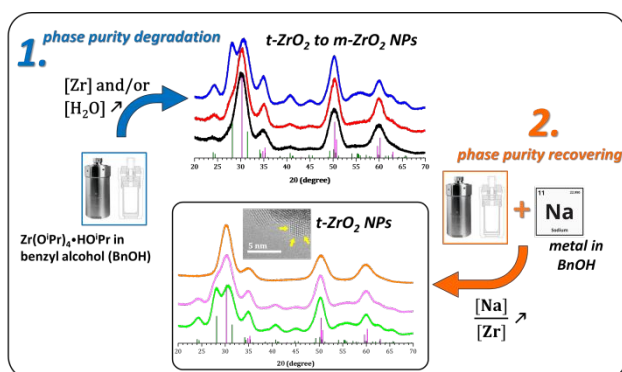
16  
17 (41) Haffad, D.; Chambellan, A.; Lavalley, J. C.; Propan-2-ol transformation on simple metal oxides TiO<sub>2</sub>,  
18 ZrO<sub>2</sub> and CeO<sub>2</sub>, *J. Mol. Catal. A, Chem.*, **2001**, *168*, 153-164.

20  
21 (42) Kozłowski, J. T.; Davis, R. J.; Sodium modification of zirconia catalysts for ethanol coupling to 1-butanol,  
22 *J. Energy. Chem.*, **2013**, *22*, 58-64.

23  
24 (43) Kyrides, L.P.; Carswell, T.S.; Pfeifer, C.E.; Wobus, R.S.; Dehydration of alcohols with alkali metal  
25 alcoholates, *Ind. Eng. Chem.*, **1932**, *24(7)*, 795-797.

27  
28 (44) Chevalier, J.; Gremillard, L.; Virkar, A.V.; Clarke, D.R.; The tetragonal-monoclinic transformation in  
29 zirconia: lessons learned and future trends, *J. Am. Ceram. Soc.*, **2009**, *92(9)*, 1901-1920.  
30  
31  
32  
33  
34  
35  
36  
37  
38  
39  
40  
41  
42  
43  
44  
45  
46  
47  
48  
49  
50  
51  
52  
53  
54  
55  
56  
57  
58  
59  
60

## For Table of Contents Only



## Synopsis:

Even under anhydrous conditions, the phase purity degradation of zirconia samples was observed jointly to the presence of water into the supernatant. Finally understood as the result of the alcohol dehydration supported by the surface of the nanoparticles and the release of in-situ water, the tetragonal-to-monoclinic transformation was inhibited by the addition of sodium metal. Indeed, the disappearance of the monoclinic phase was observed provided that a sufficient sodium-to-zirconium ratio was ensured.